

Salt Marsh Ponds as Harmful Algae Reservoirs

Authors and Affiliation:

Drs. Ling Ren, Patrick M. Gillevet & Masoumeh Sikaroodi
College of Science, George Mason University

Metthea Yepsen, Heidi O'Neill & Mihaela D. Enache
New Jersey Department of Environmental Protection

Dr. Thomas Grothues
Rutgers University

Project Manager:
Dr. Mihaela D. Enache
Division of Science and Research, New Jersey Department of Environmental Protection

March 27, 2025

Final Report to the NJ Department of Environmental Protection

Funded by the EPA Wetland Program Development Grant CD 96246800-0

State of New Jersey
Phil Murphy, Governor

Department of Environmental Protection
Shawn M. LaTourette, Commissioner



Division of Science & Research
Nicholas A. Procopio, Ph.D., Director

Visit the DSR website:
<https://dep.nj.gov/dsr>

Acknowledgments

We sincerely thank Andrea Habeck (RUMFS) for her contribution in selecting the study ponds, Thomas Grothues, Doug Douglas (RUMFS), and Lee Lippincott (NJDEP) for help with the fieldwork. We thank Kirk Raper (NJDEP) for generating the study area map and Nick Procopio (NJDEP) for the review and report improvement in both form and content.

Please cite as:

Ren, L. Gillevet, P., Sikaroodi, M., Yepsen, M., O'Neill, H., Grothues, T., and Enache, M.D. 2025. Salt Marsh Ponds as Harmful Reservoirs. Final Report to the NJ Department of Environmental Protection. Trenton, NJ. 64 Pages. Available at: <https://hdl.handle.net/10929/145921>

Table of Contents

Project Contributors	3
Executive Summary	4
Introduction	6
Materials and Methods	7
Study area.....	7
Field measurements and sample collections	9
Microalgal analysis	10
Semi-quantitative light microscopy analysis	10
Quantitative analysis.....	11
Toxin analysis	11
DNA analysis and bioinformatics.....	12
DNA extraction and purification.....	13
16S rRNA sequencing.....	13
18S rDNA sequencing	14
Bioinformatic analyses on 16S rRNA sequences.....	14
Bioinformatic analyses on 18S rDNA sequences	15
Web page development.....	15
Data analysis	15
Results	16
Environmental parameters from May 2022 to June 2023 monthly samplings	16
Monthly variations of microalgal composition from May 2022 to June 2023.....	18
Changes of microalgal composition in relation to environmental variables.....	23
DNA-based analysis on algal composition and HAB species from August 2022-June 2023.....	25
16S rRNA analysis.....	25
18S rDNA analysis	25
DNA-based classifications of HAB species.....	25
Spatial and temporal variations of DNA-based algal composition.....	29
Planktonic (surface) vs. mixed microalgal communities	29
Detection of harmful algae and biotoxins from July and August 2023	31
Environmental parameters from July and August 2023.....	31
Variations of microalgal composition from July and August 2023	31
Changes of microalgal composition in relation to environmental variables from July and August 2023.....	34
Algal biotoxins detected from July to August 2023.....	35
Webpage development.....	35
Discussion	36
Dynamics of harmful algal blooms in SMPs	36
HABs and biotoxins.....	37
Planktonic and mixed algal community.....	38
DNA-based and morphology-based classifications on HAB species	39
Summary	40
Outreach	40
Recommendations	40
References	43
Appendices	50

Project Contributors

Dr. Ling Ren, principal investigator (PI), Research Assistant Professor, College of Science, George Mason University (GMU). Project conceptualization, study design, field work, sample analysis on algae community, data analysis, outreach, and writing reports.

Dr. Mihaela D. Enache, Project Manager & co-PI, Research Scientist I, **Heidi O’Neill**, Research Scientist II, and **Metthea Yepsen**, Bureau Chief, Division of Science and Research, New Jersey Department of Environmental Protection (NJDEP). M. Enache: Project conceptualization and management, study design, field work, outreach, and reports refining. H. O’Neill: Website development. M. Yepsen: report reviewing and refining in form and content.

Dr. Patrick M. Gillevet, co-PI, Professor and Director, and **Dr. Masoumeh Sikaroodi**, laboratory manager, Microbiome Analysis Center, College of Science, George Mason University. P. Gillevet: Project conceptualization and management of DNA analysis, bioinformatics, and report refining. M. Sikaroodi: Laboratory supervision and DNA analysis method development.

Dr. Thomas M. Grothues, Co-PI, Associate Research Professor, and **Mr. Douglas Hood**, Technical staff, Rutgers University Marine Field Station (RUMFS). T. Grothues: Project conceptualization, study design, field work management, outreach, and refining report. D. Hood: Field work and data collection.

Executive Summary

Salt marsh ponds (SMPs) make up a vital component of coastal marshes. The ponds provide unique microhabitats for diverse aquatic organisms, including algae, snails, fish, crustacea, and insects; thus, they function as year-round food sources and shelters for many birds and animals that are dependent on marshes. We carried out a two-year study from May 2022 to November 2024 to investigate the temporal and spatial changes of microalgae, with a focus on harmful algae blooms (HABs) and algal/bacterial toxins in the SMPs of the marsh on the Sheepshead Meadow peninsula in Tuckerton, New Jersey. The study is based on a one-year monthly samplings for microalgae and water quality field measurements performed between May 2022 and June 2023, and three additional samplings performed July-August 2023 for HABs toxin detection. The objective of the study was to determine the presence and extent of HABs and related toxins in the SMPs. We hypothesized that the tidal SMPs can serve as inoculants of HABs and potentially function as harmful algae reservoirs and HAB sources for coastal waters.

The investigation consisted of monthly surveys on SMPs microscopic communities of algae (microalgae, henceforth) by collecting mixed samples (mixed samples, henceforth) containing both planktonic (including cyanobacteria) and benthic/epiphytic microalgae species. These samples were obtained by gently stirring the pond bottom to collect a representative microalgae sample. Alternatively, samples representing the phytoplankton communities were collected from the top 10-cm of water surface (surface samples, henceforth). Samples were collected monthly from May 2022 to June 2023 and a follow-up study took place in July and August 2023 with a focus on the detection of HAB-related biotoxins in the study SMPs. The studied six SMPs had similar pond morphology and were located in marsh areas under different mosquito control management regimes: Parallel Grid Ditching (PGD), Open Marsh Water Management (OMWM), and unaltered natural marsh. During the study, water parameters, including temperature, salinity, pH, dissolved oxygen (DO), and DO saturation (%), were measured *in situ* using a multiparameter water-quality sonde from YSI. Microalgal community composition (including HAB species) was analyzed using microscopy and DNA metabarcoding with 16S and 18S gene markers. Toxin analysis was conducted on filter samples using Enzyme-linked immunosorbent assay (ELISA) immunoassay lab testing kits.

Our investigation revealed the presence and dominant role of HAB species in the study intertidal SMPs for the first time in the Tuckerton peninsula. The extent and intensity of the HABs presence in the SMPs were remarkable. The distribution of HABs was extensive across all the ponds in the three areas of marshes in summer (June-August) and occasionally in the spring (March to May) and winter (December-January). Often, the HABs in specific ponds were characterized by extremely high abundance and dominance of one or two HAB species. In many cases, the HABs accounted for more than 60% to 98% of total algal abundance. On the other hand, the blooming HAB species across all the ponds and over the study period were highly diverse. Sixteen HAB species were recorded through microscopy observations and belonged to the groups of Diatoms, Dinoflagellates, Raphidophytes, Haptophytes, and Cyanobacteria. DNA-based analysis found higher HAB species diversity in Dinoflagellates and Cyanobacteria taxa.

Five algal toxins were detected in the SMPs, including Brevetoxin, Saxitoxin, Okadaic acid (OA), Microcystins, and Cylindrospermopsins. Furthermore, the analysis showed that multiple toxins were present simultaneously in over half of the samples. High concentration of OA (> 270 µg/L) was detected in one of the ponds at the end of July. It is worth noting that there was a decoupling between the detection of toxins and the presence of HABs under microscopy, suggesting the complexity of toxic species and toxin productions.

The study showed that water quality parameters measured over the one-year study - water temperature, salinity, pH, and DO, explain a small portion of the variance in non-harmful microalgae and HABs found in the study ponds. This implies that other factors that were not included in this study can be important contributors to these variations. Factors such as nutrients, organic matter, presence and abundance of grazers, as well as sediment type and benthic communities may play significant roles in the proliferation of HABs in the SMPs, which would require further investigations.

In addition to the mixed samples described above, a few samples were collected from the top 10-cm of surface water of each pond to explore differences in microalgal composition between these two types of samples. The diversity of taxa in the mixed samples was generally higher than that in the surface water phytoplankton, as the former contained phytoplankton, periphytic and epiphytic species, and sometimes even benthic microalgae due to the shallowness of the ponds and light penetration. The results demonstrated the ‘unevenness’ of microalgae distributions within the ponds despite the homogeneousness in physical and chemical conditions. This needs to be carefully taken into consideration when it comes to HAB and biotoxin monitoring.

A comparison of the classification and detection of HABs between the microscopy method and metabarcoding approach showed that the microscopy provided more holistic information compared to either 16S- or 18S rDNA-based metabarcoding. However, metabarcoding revealed a higher HAB diversity within certain groups when combined with specific gene markers. It is recommended that the microscopy method be supplemented with DNA-based metabarcoding for a better assessment of HABs diversity in monitoring the SMPs.

A website has been constructed to hold a total of 49 images and 21 videos illustrating 13 HAB species. For each HAB species, documentation on morphology, ecology, toxicity, distribution, and occurrence is provided. The website serves as an educational resource for the general public and students K-12 or higher about HABs in NJ coastal marshes. It also serves as an interface for connecting with NJ communities and informing them of the presence of HABs in these ponds and the potential for toxin presence. In addition, several outreach efforts were made to share the project findings through conferences, a newsletter, and a manuscript submitted to *Regional Studies in Marine Science*, currently under review.

This study demonstrated, for the first time, that HABs contribute to the dynamics of SMPs in the New Jersey coastal marshes and the presence of HAB-derived toxins in these ponds. This finding has significant implications for wetland ecology and environmental and human health. Climate change and sea level rise, through increased marsh flooding, could heighten the potential for more frequent HAB inoculation as SMPs are more regularly connected to estuarine open waters

and their fisheries. It is increasingly important to integrate SMPs into the assessment of wetland conditions, their role in HAB dynamics and effects on landcover and coastal waters.

Introduction

Coastal marshes play essential roles in ecosystem biodiversity (Greenberg et al. 2006), flood and erosion protection (Narayan et al. 2017), coastal water quality (Kennish 2001), and carbon sequestration (Rogers et al. 2019). Salt Marsh Ponds (SMPs) make up a vital component of coastal marshes and contribute to environmental and ecological significance in marsh functioning (Smith and Able, 1994, Lathrop et al. 2000, Adamowicz and Roman, 2005, MacKenzie and Dionne, 2008). They provide unique microhabitats for diverse aquatic organisms, including algae, snails, fish, crustacea, and insects, supplying year-round food sources for birds and other animals that are dependent on marshes for food and shelter. On the other hand, salt marshes globally are facing continuous loss under the stress of climate change and human activities (Campbell et al. 2022). Tidal marshes are estimated to decline by 20% to 45% in area by 2100 due to sea level rise (Craft et al. 2009), and those with more human impacts tend to experience the greatest loss (Elsey-Quirk et al. 2022).

Salt marshes in the eastern US have been extensively altered by marsh management practices for mosquito control, e.g., parallel grid ditching (PGD), open marsh water management (OMWM), and more recently, Integrated Marsh Management (IMM) (Wolfe et al. 2022). About 90% of the coastal wetlands from Maine to Virginia and 94% along New England have experienced ditching by the 1930's (Rey et al. 2012). OMWM was later developed in New Jersey by selectively excavating the ponds and ditches for more larvivorous fish habitats. The management technique was used extensively along the US Atlantic Coast. While OMWM was effective in reducing mosquitoes and more ecologically-sound (Rochlin et al. 2012), it had negative effects on marsh pond ecosystems, including water quality degradation and nekton species shifts in the ponds (James-Pirri et al. 2011). Owing to these anthropogenic modifications, storms and flooding associated with climate change, and sea level rise, the number of SMPs and their areal coverage has been overall increasing (Kirwan and Mudd, 2012). Integrating SMPs into the estimates of salt marsh habitat condition and function on both landcover and water quality has become increasingly important.

Microalgae are ubiquitous and form a major component of salt marsh food webs (Currin et al. 2003). Meanwhile, algal community composition and diversity are often indicative of environmental variabilities because of the species' habitat preferences; thus, microalgae are also considered one of the valuable indicators of the biological integrity of wetlands (USEPA, 2002). Previous studies were mostly focused on the benthic and edaphic microalgal communities beneath marsh vascular plant canopies and intertidal surfaces. These studies revealed large diversity in microalgal assemblages, with diatoms and cyanobacteria being primarily predominant (Zedler, 1980, Tracy and South, 1989, Sullivan and Currin, 2002). Diatoms are generally preferred food sources for many invertebrate and fish species in salt marshes (Sullivan and Currin, 2002) because of their high content of lipids (Sharma et al. 2016), except for many *Pseudo-nitzschia* species (Trainer et al. 2012, Fernandes et al. 2014). On the other hand, some filamentous cyanobacteria recorded in earlier studies, such as *Anabaena*, *Calothrix*, *Lyngbya*, and *Phormidium* (Tracy and South, 1989, Sullivan and Currin, 2002), could be potential toxin producers (Lassus, 2016, Nowruzi and Porzani, 2021), but this has not yet been studied in salt

marsh habitats. Studies on microalgae, including phytoplankton in coastal SMPs, are relatively sparse, and even fewer studies are focused on harmful algae and algal toxins.

A harmful algal bloom (HAB) is defined as high average phytoplankton cell density (including algae and /or cyanobacteria) occurring in a waterbody forming surface blooms that can reach up to tens of square kilometers in large lakes or oceans (Ibelings et al. 2021). HABs are a growing concern for environmental, ecological, and human health (Anderson et al. 2021). In the US, more than 11% of surface waters on Federal lands have been affected by harmful algal events, and numerous species, including marine mammals and birds, are thought to have been exposed to phytoplankton toxins (Laughrey et al. 2022). Tidal SMPs, often shallow and tidally inundated, exhibit significant differences in biogeochemistry and ecology despite similar temperature, salinity, and pond dimensions (Spivak et al. 2017). A recent study revealed significant differences in microeukaryote communities between SMPs, and the presence of several harmful microscopic algae in the coastal marshes of New Jersey (Potapova et al. 2024). However, their study was limited to one sampling event and did not cover spatial and temporal distributions of microalgae and HAB species in the SMPs.

The objective of this study was to determine the presence and extent of harmful microalgae and toxins in the SMPs. We hypothesize that the tidal SMPs, which form unique microhabitats, can serve as inoculants of HABs and potentially function as harmful algae reservoirs and sources for coastal waters. We carried out a two-year study from May 2022 to November 2024 to investigate the temporal and spatial changes of microalgae in the SMPs of different marsh types on the Sheepshead Meadow peninsula in Tuckerton, New Jersey, with a focus on HABs and related toxins. The investigation consisted of monthly surveys on water parameters and microalgal communities in 6 SMPs from May 2022 to June 2023. Water parameters, including salinity, water temperature, pH, specific conductivity, and dissolved oxygen, were measured in the field. The microalgal community composition was analyzed using microscopic semi-quantitative method and Next-Generation DNA sequencing to lowest taxonomic level (species or variety) when possible.

A follow-up study was carried out in July and August 2023 with a focus on the detection of HAB species and toxins. Three field trips were made during the two months. All six SMPs were revisited, and water parameters were measured *in situ*. The microalgal species composition was analyzed using light microscopy, and HAB biotoxins were detected using ELISA.

This report presents results from this study, including water parameter measurements and microalgal community compositions, the temporal and spatial distributions of HABs, their potential relationships to measured parameters, biotoxins detected in the SMPs, and the website developed to illustrate HABs found in the SMPs.

Materials and Methods

Study area

The Sheepshead Meadow peninsula is a marsh platform located within the Jacques Cousteau National Estuarine Research Reserve (JC NERR), a NOAA designated sentinel site, encompassing the Mullica River – Great Bay estuary to the south and Little Egg Harbor, part of the Barnegat Bay estuarine complex, to the north (Kennish et al. 2014). A sentinel site is a marine or coastal area sanctuary where research and monitoring are conducted to understand and

protect the ecosystem. The northwestern segment of the peninsula was ditched through PGD in the 1920s, and the central segment was modified through OMWM from the 1960s to the 1990s. The southern segment of the peninsula, however, remains one of the largest unaltered salt marshes in NJ (Fig. 1). A previously conducted spatial analysis showed different spatial patterns of the land-water interface under different management regimes (Lathrop et al. 2000). In general, the PGD segment has a lower number of SMPs and a higher ratio of marsh surface-to-tidal water interface. In comparison, the OMWM segment has a greater density of SMPs.

A previous study showed the differences in marsh plant species composition, abundance, and structure between the northern PGD, the OMWM, and reference segments (Meixler et al. 2018). For instance, the PGD segments had a higher abundance of high marsh species (i.e., *Spartina patens* and *Distichlis spicata*) than the central or southern segments. Moreover, salt marsh pools (ponds) in the marshes on the Tuckerton peninsula serve as winter refuges for the fish, favoring ponds over subtidal and intertidal creeks (Smith and Able, 1994), and provide critical habitats for diverse fish communities, for spawning and at multiple life stages (Able et al. 2005). However, little is known about microalgae in marsh habitats in this area.

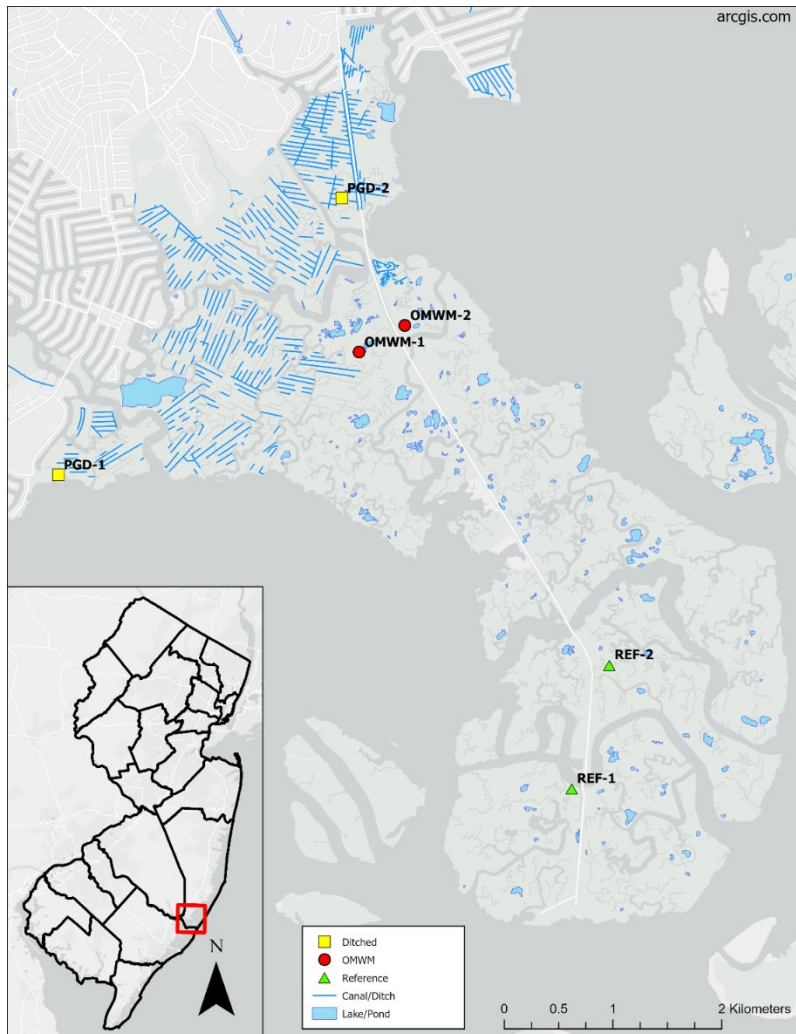


Fig. 1. Map of the study area: Sheepshead Meadow peninsula, Tuckerton, New Jersey, showing three segments with different alteration histories, including PGD (parallel grid ditches), OMWM (open marsh water management), and REF (reference, un-altered). Two study ponds were selected in each segment. Map metadata description: [National Hydrography Dataset \(NHD\) Waterbody 2015 for New Jersey - Overview \(arcgis.com\)](#) (Map produced by Kirk Raper, at New Jersey Department of Environmental Protection)

Field measurements and sample collections

Two SMPs were selected, based on pond size and morphology, surroundings, salinity, tidal effects, and accessibility, in each of the three segments of the Sheepshead Meadows peninsula: the PGD-modified northwest segment, the OMWM-modified central segment, and an un-altered reference area (REF) located in the southern segment of the peninsula (Table 1, Fig. 1). The selected SMPs were visited every month from May 2022 to June 2023 for field water parameter measurements and algal collections. The fieldwork was consistently done at low tide in consideration of accessibility. Storm and heavy rain events were avoided owing to the excess disturbance of pond waters. Water parameters, including temperature, salinity, pH, conductivity,

dissolved oxygen (DO) concentration, and DO saturation (DO%), were measured in the field using a YSI Environmental Data Logger Professional Plus (Pro Plus) and Quatro field cable (Yellow Springs Instruments, Yellow Springs, Ohio). To test the homogeneity of pond water, measurements were taken from three locations in each pond in December, February, and June. The instrument was cleaned and calibrated following the manufacturer protocols the day prior to each field trip and rinsed between each pond.

Table 1: Locations and dimensions of the study salt marsh ponds (SMPs) on Sheepshead Meadows peninsula in Tuckerton, New Jersey.

Site ID	Description	Latitude	Longitude	Size (m)	Depth (m)
REF-1	Un-altered (reference) area. Site 1	39°31'10.00"N	74°19'13.37"W	12×15	0.6
REF-2	Un-altered (reference) area. Site 2	39°31'46.83"N	74°18'58.81"W	12×19	0.8
OMWM-1	Open marsh water management (OMWM). Site 1	39°33'20.12"N	74°20'34.94"W	20×25	0.5
OMWM-2	Open marsh water management (OMWM). Site 2	39°33'28.07"N	74°20'17.31"W	18×20	0.4
PGD-1	Parallel grid ditching (PGD). Site 1	39°32'43.69"N	74°22'30.76"W	8.5×12	0.4
PGD-2	Parallel grid ditching (PGD). Site 2	39°34'6.09"N	74°20'41.47"W	14×24	0.4

Microalgal samples were collected from each pond after the water parameter measurements. Prior to collecting, the pond water was stirred gently to mix phytoplankton with the algae attached to macrophytes and surface sediment, and a mixed sample was collected. In spring and summer, phytoplankton samples were also collected from the surface water to ~10 cm depth without stirring the pond water.

For each phytoplankton sample, about 50-100 ml subsample was filtered through 0.7 um pore-size polycarbonate membranes and the membranes were immediately frozen for Next-generation DNA sequencing. An unpreserved subsample was used for initial scanning under a microscope and image and video documentation. In addition, another subsample of ~100 ml was preserved with glutaraldehyde to a final concentration of 1% (v/v) and was used for semi-quantitative light microscopy analysis and quantitative analyses. In the follow-up 2023 toxin detection study, about 100 ml water samples were filtered through the same type of 0.7 um pore-size polycarbonate membrane. The membranes were then frozen at -30°C prior to the analysis.

Microalgal analysis

Semi-quantitative light microscopy analysis

A semi-quantitative light microscopy analysis method was used to analyze the whole phytoplankton community in monthly samples collected from May 2022 to June 2023. For each sample, microscopy examinations were performed on the preserved water samples for taxonomic

identifications and biovolume estimation of the dominant and abundant taxa, using a semi-quantitative method adapted from Bahls (1993). A few drops of water sample were spread evenly onto a clean glass slide and covered with a clean cover slip (“wet mount” hereafter). The wet mount was then scanned under a microscope Leica DML 2 at the magnification of 100x for overall observation, then at 400x for identifying and ranking. All encountered taxa were identified during the examination and their abundance was ranked from 1 (rare) to 5 (highly abundant) according to the criteria in Table 2. Examinations were repeated on additional wet mounts from the same sample in an iterative process until scanning of a new wet mount yielded few or no new taxa. The biovolume percentage of each non-rare taxon was estimated based on the abundance rating and cell sizes to total 100%.

Table 2: Abundance rating scales following Bahls (1993) for micro-algae in the samples collected from salt marsh ponds (SMPs).

Abundance Rating (micro algal component)
1 (rare) Observed only once or twice during the analysis
2 (occasional) Observed several times during the analysis but not in every view field of the microscope
3 (common) Observed, but less than 5 times in every view field during analysis
4 (abundant) Observed several times (5-10) in every view field during analysis
5 (highly abundant) Observed many times (10-40) in every view field during analysis

Quantitative analysis

Quantitative analysis was used to quantify the HAB species in the monthly samples collected during the study period from May 2022 to June 2023. It was also used to analyze the whole algal community composition, including HAB species, in the samples collected during the toxin study in July and August 2023. The quantitative counting was performed using a Palmer-Maloney cell following the Manuals and Guides by the Intergovernmental Oceanographic Commission (IOC) (LeGresley and McDermott, 2010). A 0.1 ml volume of preserved sample was dispensed to the counting cell, and the taxa were counted under a microscope Leica DML 2 at a magnification of 200×. The detection limit of the method is 10 cells/ml.

Toxin analysis

Toxin analysis was conducted on mixed and surface water samples collected in July and August 2023. An additional sample collected in May 2017 from OMWM-1 was also analyzed for biotoxins. Samples were rapidly screened under the microscope and the ones found with “abundant” HAB species were filtered through a 0.4 µm pore-size membrane. The filters which retained the HAB cells were shipped to Beacon Analytical Systems Inc. for analysis of biotoxins including Brevetoxins (Catalog No. 20-0200), Saxitoxins (Catalog No. 20-0173), Okadaic acid (Catalog No. 20-0184), Microstins (Catalog No. 20-0068), and Cylindrospermopsins (Catalog

No. 20-0149-N), using ELISA immunoassay lab testing kits. More information about test procedures can be found at <https://www.beaconkits.com/products>.

DNA analysis and bioinformatics

Several steps were taken to analyze the filter samples for microalgae and cyanobacteria classification and composition. These steps include DNA extraction and purification, polymerase chain reaction (PCR) amplification, LH-PCR (length heterogeneity PCR) fingerprinting (a method capable of distinguishing amplicons originating from different organisms), and multitag Next- Generation Sequencing (a method where multiple unique tags are attached to DNA fragments allowing for simultaneous analysis of biological samples). Amplicons are segments of DNA or RNA obtained by replication and amplification through polymerase chain reaction (PCR). Fingerprinting is a lab technique that allows one to distinguish organisms through the analysis of specific segments of their DNA. Bioinformatic analyses were carried out using RDP 11 (Ribosomal Database Project) and BLASTn (Basic Local Alignment Search Tool). A schematic diagram of the molecular analyses on phytoplankton samples is illustrated (Fig. 2).

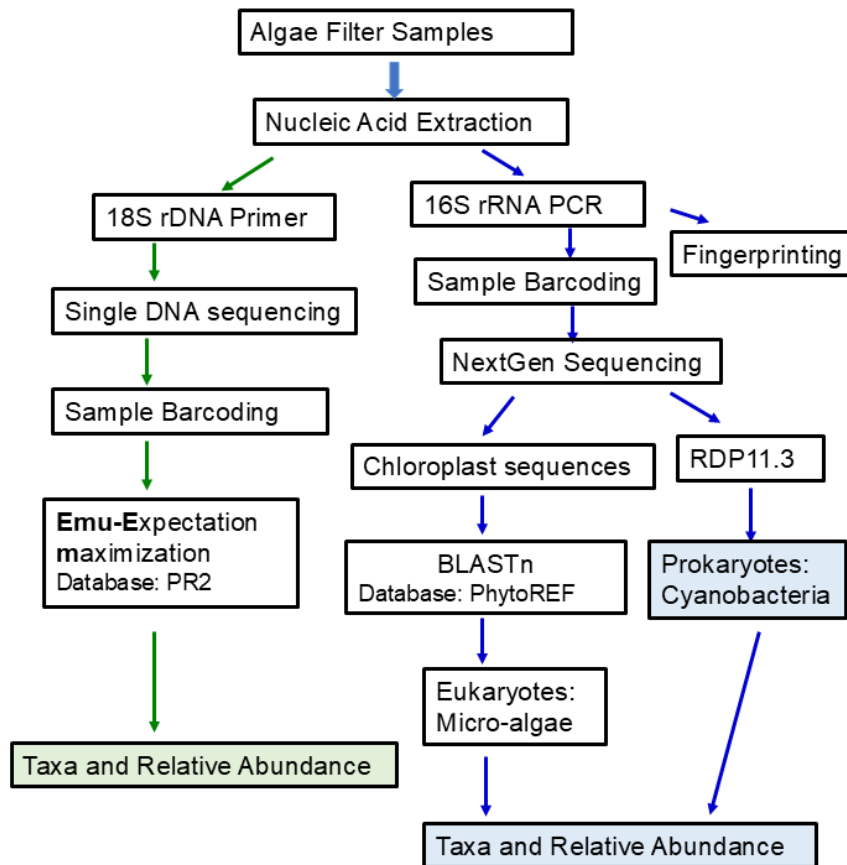


Fig. 2. Schematic diagram of the molecular work on phytoplankton metabarcoding.

DNA extraction and purification

Total genomic DNA was extracted from filter samples using “BIO101-FastDNA Spin Kit for Soil” made by MP Biomedicals Inc., Montreal, Quebec as per the manufacturer’s instructions. A dilution of the DNA was made (usually 1:5 dilution with 0.1X TE buffer) to avoid freeze-thawing the samples. The original DNA is kept at -80 °C freezer for long-term storage.

16S rRNA sequencing

PCR amplification and LH-PCR fingerprinting

DNA fragments were then amplified by polymerase chain reaction (PCR) with a universal 16S rRNA primer, 27F forward (5’AGAGTTTGATCMTGGCTCAG3’) and 355R reverse (5’ACTCCTACGGGAGGCAGC3’). Duplicate PCR was done to test the dilution and optimize the conditions for different samples. Some samples had to be diluted further (to 1:10 or 1:100), while for others, the original DNA concentration was retained. The PCR products were visualized with ethidium bromide and diluted with diH₂O from 1:10 to 1:30 of ratios based on their intensity and then added to ILS-600 (internal lane standard from Promega) and HiDi formamide (Applied Biosystems) mix in 1:10 ratio (1-part diluted PCR product and nine parts ILS mix). ILS-600 and HiDi Formamide mixture was made in a 1:20 ratio (one-part ILS600 and 19 parts HiDi Formamide). The mixture was run on a capillary electrophoresis instrument (ABI3130XL) for fingerprinting and comparing the complexity of the community by determining the size of the OTU (Operational Taxonomic Unit) peaks. Duplicates or triplicates were done on each DNA sample to compare the replicability and consistency of the PCR results. The fingerprinting was done as quality control to determine the reproducibility and reliability of the PCR. The fingerprint results were analyzed and visualized using Genemapper v4.1 software (http://tools.thermofisher.com/content/sfs/manuals/cms_070157.pdf).

Multitag Next-Generation (NextGen) sequencing

Multitag NextGen sequencing was done on the samples that worked best in PCR amplifications. The step generated a set of 96 emulsion PCR fusion primers that contain the Ion Torrent emulsion PCR linkers and different 8 base “barcode” on either the 27F or 355R of universal 16S rRNA primers (Gillevet et al. 2010). Each sample was amplified with a uniquely barcoded set of forward and reverse 16S rRNA primers. Both primers have specific adaptors to use with Ion Torrent technology and the forward primers have a barcode (or tag) incorporated into the primer sequence to be able to differentiate the sequences in different samples. Up to 48 samples were pooled and the sample pool was purified using Ampure solution (Beckman Coulter) to remove any primers or extra nucleotides. After quantitating the purified products, the NextGen sequencing was performed using Ion Torrent technology (Life Technologies) following the manufacturer’s protocols (http://tools.thermofisher.com/content/sfs/manuals/MAN0007273_IonPGMSequenc_200Kit_v2_UG.pdf). Data from each pooled sample was “deconvoluted” by sorting the sequences into bins based on the barcodes using custom PERL scripts, to normalize each sample by the total number of reads from each barcode. The data was initially analyzed with Ion Torrent software which produces a FASTQ file. A FASTQ file is a text format file used to store raw sequence data in bioinformatics. A Perl script was written to de-multiplex (separate sequencing reads into individual samples) the sequences and to assign the correct IDs to samples based on the barcodes (or tags). The resulting FASTA file (text-based file storing the biological sequences in

bioinformatic format for further analyses) was uploaded into Galaxy portal on the Microbiome Analysis Center (MBAC) website (<http://mbac.gmu.edu>) for further analyses.

18S rDNA sequencing

DNA samples were sequenced using Oxford Nanopore technology through the Nanopore Flongle analysis pipeline, which sequences single DNA molecules as they pass through a pore in an artificial charge clamped membrane. We applied state-of-art technology (Kerkhof et al. 2017) to sequence the key informative regions of the 18S rRNA gene, using the primer pairs ‘euk18S’, euk-A7F forward (AACCTGGTTGATCCTGCCAGT), and euk-570R reverse (GCTATTGGAGCTGGAATTAC) (Esenkulova et al. 2020). The Oxford Nanopore Rapid Sequencing Kit SQK_RPB114.24 and Flongle Expansion kit EXP_FSE001 were used to run the amplified products on the Flongle. This work was done on a PC with a NVIDIA GPU board (RTX A400) which has 6,144 CUDA cores to allow base calling in real-time.

Bioinformatic analyses on 16S rRNA sequences

Bioinformatic analyses on 16S rRNA sequences were carried out using RDP 11.3 (Ribosomal Database Project) and BLASTn (Basic Local Alignment Search Tool) for taxonomic classification and relative abundance of each sample.

RDP 11.3 analysis

Ribosomal Database Project (RDP) 11.3 (<https://sourceforge.net/projects/rdp-classifier/>) was used to analyze rRNA gene sequences for taxonomic classification and relative abundance of each taxon (Cole et al. 2013). RDP is a curated online database that provides annotated ribosomal RNA (rRNA) sequences and analysis tools to identify microorganisms through 16S rRNA sequences. The relative abundance of the taxa was calculated using a custom PERL script (a high-level, open-source language program) and taxa present at > 0.1% of the community were tabulated. The OTUs constituting less than 0.1% of the total community from each sample were eliminated from the analysis, with a priori assumption that the low abundance components of the community vary between individual subjects and do not contribute significantly to the functionality of the whole community. In RDP 11.3 analysis, the classification with a correlation bootstrap greater than 0.60 is considered a ‘true’ identity, the classification with a bootstrap between 0.60 and 0.10 is noted with ‘other,’ and those with bootstrap less than 0.10 are classified as ‘unknown.’ The standard nucleotide BLASTn analysis was performed on 16S rRNA sequences against the GenBank 16S Microbial Database at the National Center for Biotechnology Information (NCBI) (<https://blast.ncbi.nlm.nih.gov/>). The non-redundant nucleotide database ‘Nucleotide Collection (nr/nt)’ was selected for taxonomic classification (Zhang et al. 2000) with exclusion of uncultured/environmental sequences. Prokaryotic communities, including bacteria and cyanobacteria, were identified at the taxonomic levels of genus, species, and strains. The taxa with relative abundance >0.1% of the whole community were analyzed and presented in the results.

BLASTn analysis against PhytoREF

BLASTn is a Basic Local Alignment Search Tool (BLAST) used to compare a nucleotide (DNA) sequence to a database of nucleotide sequences. We tested the applicability of using the 16S rRNA gene as a taxonomic marker for the classification of autotrophic organisms (Yoon et al. 2016, Bennke et al. 2018). The BLASTn analysis was carried out against an online database PhytoREF (<http://phyto-ref.sb-roscoff.fr/>; accessed January 2024). The database contains 6490

plastidial 16S rDNA reference sequences from a large diversity of eukaryotes representing all known major photosynthetic lineages. It includes 6490 plastidial 16S rDNA reference sequences originating from a large diversity of eukaryotes representing all known major photosynthetic lineages. The database also contained 554 cyanobacteria classifications, and most of the classification is to the family or genus level (Decelle et al. 2015).

Bioinformatic analyses on 18S rDNA sequences

The 18S full length reads were trimmed using the Barcode trimmer in the MinKnow software (<https://nanoporetech.com/document/experiment-companion-minknow>) package and converted to MBAC format. MBAC data files are formatted based on a specific code to allow further analysis of microbiome data. The MBAC data file was used to track the Sample-ID with each Read-ID using a custom PERL script. Data is then transferred to a 48 core, 3TB memory HP (Hewlett-Packard) server.

The reads were then processed using *Emu*, which is a microbial community profiling software tool (<https://gitlab.com/treangenlab/emu>) tailored for full-length ribosomal RNA data (Curry et al. 2022). *Emu*'s algorithm involved a two-stage process. First, proper alignments were generated between reads and the supplied reference database using minimap2. The PR2 database (Guillou, 2013, Vaalot et al. 2022), used as a reference database for this study, was formatted to be compatible with the *Emu* data structure (Curry et al. 2021) using a custom PERL script. PR 2 (Protist Ribosomal Reference) database ecosystem is a set of three interconnected 18S rRNA databases used in metabarcoding. Then, as the second stage, the Expectation-Maximization (EM) based error-correction is performed to iteratively refine species-level relative abundances based on total read-mapping counts. This method provides microbial community profile estimations from full-length DNA sequence reads, which are more accurate than existing methods at both the genus and species level. We then used a custom PERL script to parse the two *Emu* output files to construct sample abundance tables for each of the taxonomic levels down to the species level.

Web page development

A project webpage was developed using WordPress Version 6.5.5 to share the project findings on harmful algae. The documentation on HAB species consists of images and videos recorded from the microscopic observation and their potential toxicity and ecological characteristics based on published literature ([repository of the detected species](#)).

Data analysis

Ordination analyses were performed to calculate the similarity (dissimilarity) among different samples in terms of algal community composition with the exclusion of 'rare' taxa (see Table 2). Sample distances were calculated using the Bray-Curtis distance measure. Nonmetric Multidimensional Scaling (NMDS) was performed and rotated using Principal Components Analysis. The rotation step maximizes the variation of case scores along NMDS axes. Diagrams of sample ordinations were constructed in two dimensions, in which the relative distance between samples reflects the relative similarity in community composition.

Canonical Correspondence Analysis (CCA) quantified the relationship of beta diversity in the microalgal community with environmental variables. Biovolume composition of microalgae excluding 'rare' taxa (see Table 2) was used for the analysis. Conductivity and DO saturation were excluded from the analysis due to their strong covariance with salinity and DO

concentration, respectively, following concerns about over-parameterization (King and Jackson, 1999). CCA analysis thus included four environmental parameters: water temperature, salinity, pH, and DO concentration. All statistical analyses were performed using the software Canoco 5 (ter Braak and Šmilauer 2012).

Results

Environmental parameters from May 2022 to June 2023 monthly samplings

Monthly measurements of salinity, temperature, pH, and dissolved oxygen (DO) from May 2022 to June 2023 are shown in Fig. 3.

Salinity and water temperature showed strong seasonal variations in each pond. The highest temperature reached a little over 30°C in August 2022 and was slightly below 10°C during winter. In mid-March 2023, a cold front resulted in a temperature decrease to around 5°C. Spatially, the temperature was very similar among the ponds most of the year and slightly variable, < 3°C difference, in summer and winter (Fig. 3a). Salinity was weakly seasonal and ranged 25-45 ppt in summer and 25-31 ppt in winter. The extreme high salinity of ~45 ppt was detected in OMWM-2 in August 2022. The differences among the ponds were usually < 5 ppt (Fig. 3b). The REF ponds showed less fluctuation throughout the year compared to others. Higher salinity in summer (~ 35 ppt) may have resulted from high heat-induced evaporation and relatively small water volumes in the ponds.

The pH values showed slight seasonality with generally higher summer and lower winter values and fluctuated more in warm months from April to September in all the ponds. Typically, pH ranged between 7.3 to 8.6, but extremely high values of 9-9.7, were detected in OMWM-2 and OMWM-1 during summer, and low values of 6.9-7.0, in PGD-1 in May 2022 and April 2023 (Fig. 3c). The DO concentration fluctuated among months without strong seasonality. Typically, DO measurements varied between 6 to 14 mg/mL, but some extremely high values (> 18-20 mg/L) were detected in OMWM-1 and 2, and low concentrations ~2 mg/L in PGD-1 in May 2022 and REF-1 in April 2023 (Fig. 3d).

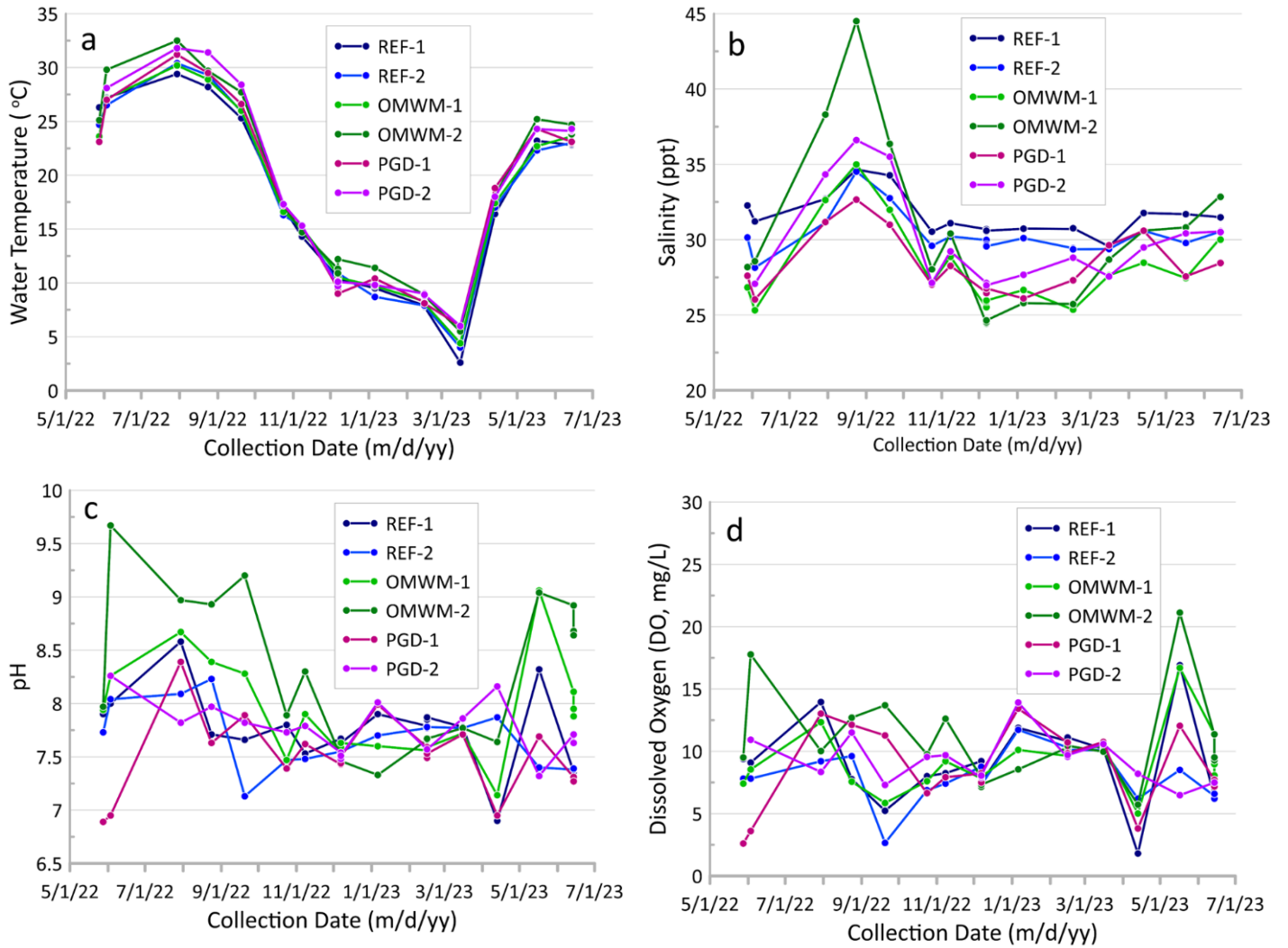


Fig. 3. Monthly measurements of water temperature, salinity, pH, specific conductivity, dissolved oxygen (DO), and DO saturation in the salt marsh ponds (SMPs) on the Sheepshead Meadow peninsula in Tuckerton, New Jersey, from May 2022 to June 2023.

Significant linear correlations were obtained between salinity and conductivity (Fig. 4a), and dissolved oxygen (DO) concentration and DO saturation (Fig. 4b).

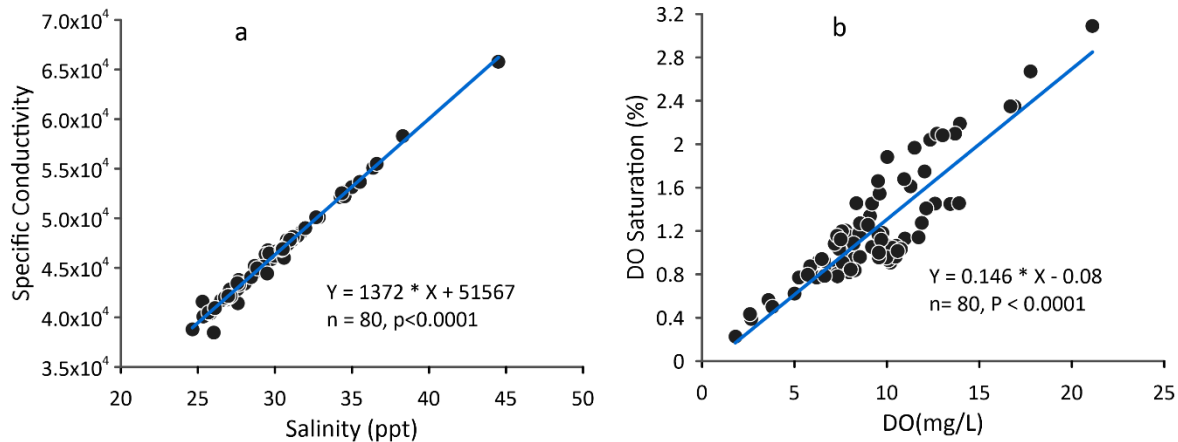


Fig. 4. Correlations between salinity and conductivity (a), and dissolved oxygen (DO) concentration and DO saturation (b) in the SMPs from May 2022 to June 2023

The environmental variables measured in 3 locations within each pond were homogeneous as indicated by the standard deviation and coefficient of variation from the replicate measurements taken in December, February, and June (Table A1).

Monthly variations of microalgal composition from May 2022 to June 2023

Fig. 5 shows the compositions of taxa identified in the SMPs from May 2022 to June 2023, based on semi-quantitative microscopy analysis. In addition, the taxa encountered as ‘occasional’ to ‘highly abundant’ in at least one sample and their occurrences are listed in Table A2.

The temporal and spatial variations of the mixed samples compositions were highly dynamic during the study period of May 2022-June 2023. In each pond, the dominance of specific taxonomic groups, particularly diatoms vs. non-diatoms, changed successively (Fig. 5). Diatoms dominated fall assemblages from September to November of 2022 in most of the ponds. In the following months, the succession of microalgal groups changed quickly within each pond and differed between ponds. In REF-1, diatom percentages decreased in December 2022-January 2023 and increased again from February until May-June 2023, accounting for 61% to 97% of the total microalgal community during that time. In comparison, diatom percentages in REF-2 decreased to 20% in February due to green algae growth and increased again to >50% from March through June of 2023. In PGD and OMWM ponds, diatoms contributed most to the winter and spring assemblages, especially in PGD-1 and OMWM-1, while green algae and dinoflagellates became abundant and dominant during summer and fall in these ponds. In

OMWM-2, dinoflagellates were dominant most of the study period. During July-August 2022, dinoflagellates, raphidophytes, or cyanobacteria dominated the microalgal communities.

Within each taxonomic group, species succession was different among ponds (Table A2). For example, diatoms were dominant in REF-1 in October-November (fall) and March-April (spring) as shown in Fig. 5. However, fall diatoms were composed of *Gyrosigma*, *Pleurosigma*, and Naviculoids, whereas the spring diatoms had an abundance of *Haslea ostrearia*. With few exceptions, most diatoms are nontoxic. The toxin-producing *Pseudo-nitzschia* species was detected 'occasional' in December and January in REF-1, PGD-1, and OMWM-1. A harmful diatom, *Cylindrotheca closterium*, was abundant from April to June of 2023 in all SMPs.

Most dinoflagellate species are toxic and harmful. *Akashiwo sanguinea*, *Kryptoperidinium foliaceum*, *Levanderina fissa*, *Gymnodinium aureolum*, and *Prorocentrum lima* dominated the summer assemblages in REF-1, PGD-1, PGD-2, and OMWM-2 (Table 3), accounting for 60-93% of total biomass. In winter, algal abundances were generally low compared to the summer, while dinoflagellates, mainly *P. lima* (Table 3 and Table A2), were still 'abundant' and dominant in December - January, making up to 60% and 98% of total biomass in PGD-2 and OMWM-2, respectively. Moreover, *P. lima* made up to 40-90% of the algal community in OMWM-2 in March-May 2023. Two toxin-producing raphidophyte species, *Chattonella subsalsa* and *Heterosigma akashiwo*, were 'highly' abundant in PGD-2 in July and OMWM-2 in August 2022, respectively. Co-existence of both species was observed in high abundance in PGD-2 also in August 2022.

Cyanobacteria were present frequently in various ponds throughout the year. The highest percentage of cyanobacteria was detected in OMWM-1 in early June 2022, accounting for 65% of total phytoplankton, and composed of *Lyngbya aestuarii* and *Planktothryx agardhii*, both being potential toxin producers. Other cyanobacteria such as *Chroococcus* and pico-coccoical *Aphanocapsa* species were common but rarely 'abundant' or dominant. Another harmful cyanobacterium, *Phormidium autumnale* was 'abundant' in OMWM-2 in February 2023 (Table S1). The golden alga *Prymnesium parvum* was 'abundant' in PGD-2 in April and dominant in OMWM-1 in May 2023 (Fig. 5), reaching extremely high cell density $> 8 \times 10^5$ cells/ml.

Differences in microalgal communities between two ponds located in the same type of segment area were observed (Fig. 5). In August 2022, REF-1 was dominated by dinoflagellates, whereas REF-2 was characterized by highly abundant raphidophytes. There were differences also between PGD-1 and PGD-2 in July 2022 and April 2023. In May 2023, the golden alga was dominant in OMWM-1 while dinoflagellates dominated OMWM-2 (Fig. 5). The differences were also detected at the species/genus level. In April 2023, diatoms were dominant in both REF ponds, however, REF-1 was dominated by *Haslea ostrearia* (90% of total biomass estimate), a diatom with blue pigment, whereas REF-2 was 'abundant' with several other diatoms including *Striatella unipunctata* and *Melosira moniliformis*. At the end of July 2022, dinoflagellates became abundant in REF-1&2, PGD-1 and OMWM-2, however, each pond held different dinoflagellate species. In REF-1, *A. sanguinea* was dominant and accounted for 85% of the assemblage, while REF-2 was characterized by a mix of 'abundant' *A. carterae*, *P. lima* and *A. sanguinea*. Meanwhile, PGD-1 was populated by *K. foliaceum* (55%), and OMWM-2 by *G. aureolum*.

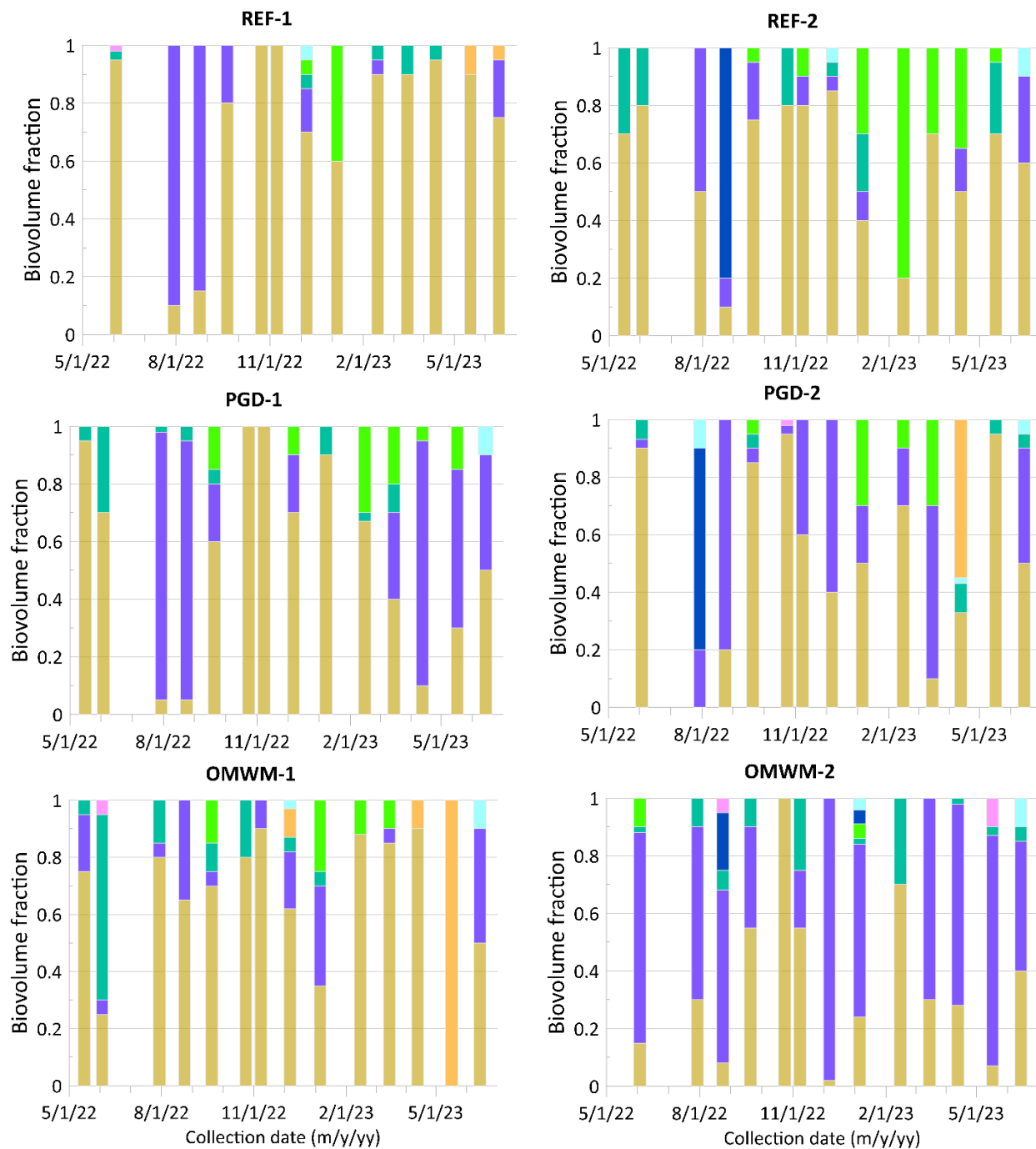


Fig. 5. Monthly composition of microalgal communities in the SMPs on Sheepshead Meadow peninsula, Tuckerton, New Jersey, from May 2022 to June 2023. Groups with HAB species: Dinoflagellates: multiple species; Cyanobacteria: *Planktothryx agardhii*, *Phormidium autumnale*, and *Lyngbya aestuarii*; Raphidophytes: *Chattonella. subsalsia* and *Heterosigma. akashiwo*; Haptophytes: *Primnesium parvum*. See Table 3 and A2 for details.

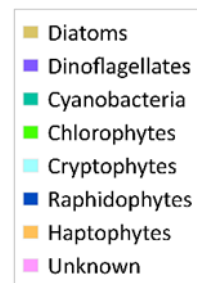


Table 3: Harmful algal bloom (HAB) species occurrence, maximum cell density and potential toxins and toxicity. Months and SMPs in bold indicate that the HAB species were detected at ‘abundant’ or ‘highly abundant’ densities (See Table 2).

Species	Months	SMPs	Maximum cell density (cells/mL)	Toxins & Toxicity
Dinoflagellates				
<i>Prorocentrum lima</i>	Dec-Jan, Apr- May, Jun-Aug, Sept	REF-2, OMWM-1, OMWM-2	6.7×10^4	Okadaic acid; Diarrheic shellfish poisons (DSPs)
<i>Amphidinium carterae</i>	Dec-Mar, Jun-Sept	OMWM-1, PGD-2	0.8×10^3	Hemolysins; Ciguatera fish poisons (CFP)
<i>Akashiwo sanguinea</i>	May, Jun, Jul, Nov	REF-1 & 2 PGD-1 & 2	1.04×10^4	Ichthyotoxic, cause gill-clogging; suffocation due to low oxygen
<i>Gymnodinium aureolum</i> (<i>Karlodinium</i> sp.)	April-Aug, Sept	REF-1, PGD-1&2	5.7×10^3	Karlotoxins, polyketide toxins
<i>Levanderina fissa</i> (syn. <i>Gyrodinium uncatenum</i>)	June, July, Aug	REF-1, OMWM-2, PGD-1&2	1.8×10^4	Toxin unknown; Ichthyotoxic effects; blooms related shrimp kills
<i>Kryptoperidinium foliaceum</i> (syn. <i>Peridinium foliaceum</i>)	May-Aug	PGD-1 & 2 OMWM-2	2.7×10^4	Cause metabolic stresses
Cyanobacteria				
<i>Planktothrix agardhii</i>	Jan, Apr, Jun, Nov	REF-1 & 2, PGD-2, OMWM-1 & 2	0.2×10^3 (as # of filaments)	Microcystins; Hepatotoxins; possible human carcinogen
<i>Phormidium autumnale</i>	Feb	OMWM-2	0.6×10^3 (as # of filaments)	Anatoxin-a; Neurotoxic shellfish poisons (NSP)
<i>Lyngbya aestuarii</i>	May, Jun	PGD-1 & 2, OMWM-1&2	8×10^3 (as # of filaments)	Multiple toxins: lyngbyatoxin A and debromoaplysiatoxin; cause irritation on skin, eyes and respiratory system
Haptophyte				
<i>Prymnesium parvum</i> (“golden alga”)	Apr, May Jun	REF-1 & 2, PGD-2 OMWM-1 & 2	8.5×10^5	Prymnesins; Cytotoxic, hemolytic, neurotoxic and ichthyotoxic poisons
Raphidophytes				
<i>Chattonella subsalsa</i>	Jun, Aug, Nov	REF-2, PGD-2, OMWM-2	8.8×10^3	Brevetoxins and hemolytic substance, NSP
<i>Heterosigma akashiwo</i>	Jul, Aug	REF-1, PGD-1 & 2	1.4×10^4	Brevetoxins and hemolytic substance, NSP

Community differences were also visible in the NMDS ordination diagram (Fig. 6). Seasonal variations were evident in most ponds, as indicated by the distances between samples in the ordination. In general, the June-August summer assemblages were distinct from those in the cold months. Abundant taxa could be comparable among all ponds but dominate at separate times, creating a spatial-temporal mosaic that left ponds similar overall but dissimilar during the same month sampling event (Fig. 6, lower panel). In an exception, the OMWM-1 sample from May 2023 (labeled as O10523 in Fig. 6, upper panel) was highly distinct from other samples attributed to the absolute dominance of *P. parvum*.

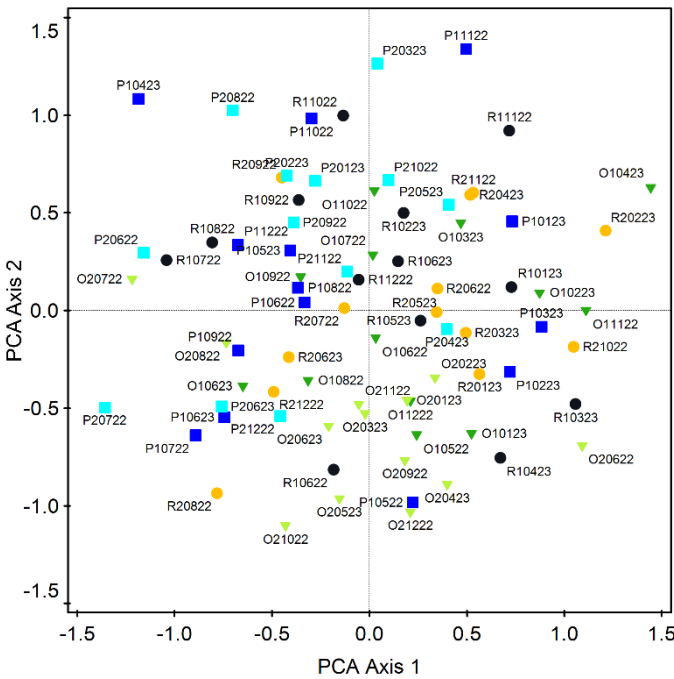
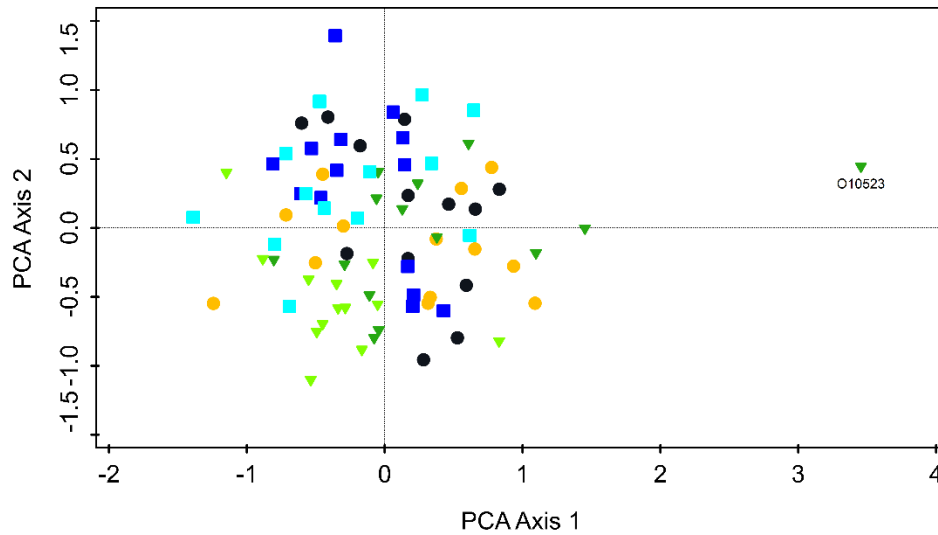
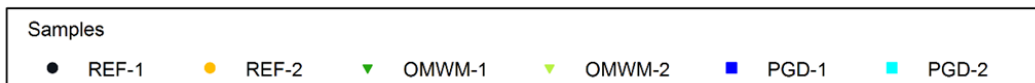


Fig. 6 Variability of algal community among the salt marsh ponds (SMPs) from May 2022 to June 2023 based on non-metric multidimensional scaling (NMDS). SMP sites are color coded. Each sample is labeled with the codes of site (initial letter with 1 or 2), collection month (MM, the 3rd and 4th digits), and collection year (YY, last 2 digits). The scaling is focused on sample scores, and the distance between the symbols approximates the dissimilarity of algal communities as measured by the Euclidean distance. Upper panel ordination includes sample O10523, and lower panel ordination without sample O10523



Changes of microalgal composition in relation to environmental variables

Water temperature and pH were the most significant factors (of the examined) related to microalgal community composition ($p < 0.01$), followed by salinity and DO, as shown by CCA analysis (Fig. 7). These four parameters explained about 6.9% of the total variation of the algal community. The associations of species occurrences and successions were correlated to the environmental parameters as indicated by the distances between species and the species projections to the environmental arrows in Species-Environment biplot (Fig. 8). Diatoms, such as *Melosira*, *Gyrosigma*, *Skeletonema* and tube-dwelling *Navicula* sp. were more frequent in cold seasons, whereas summer diatoms included *Entomoneis*, *Fragilaria*, and *Rhopalodia*. The HAB species, *A. sanguinea*, *K. foliaceum*, and *G. uncatenum* (syn. *L. fissa*), and *C. subsalsa* and *H. akashiwo* were correlated with the temperature gradient and highly abundant in summer while *P. lima* appear to prefer lower temperatures. *P. parvum* and *L. aestuarii* were less correlated with temperature but showed affinity for high pH (Fig. 8).

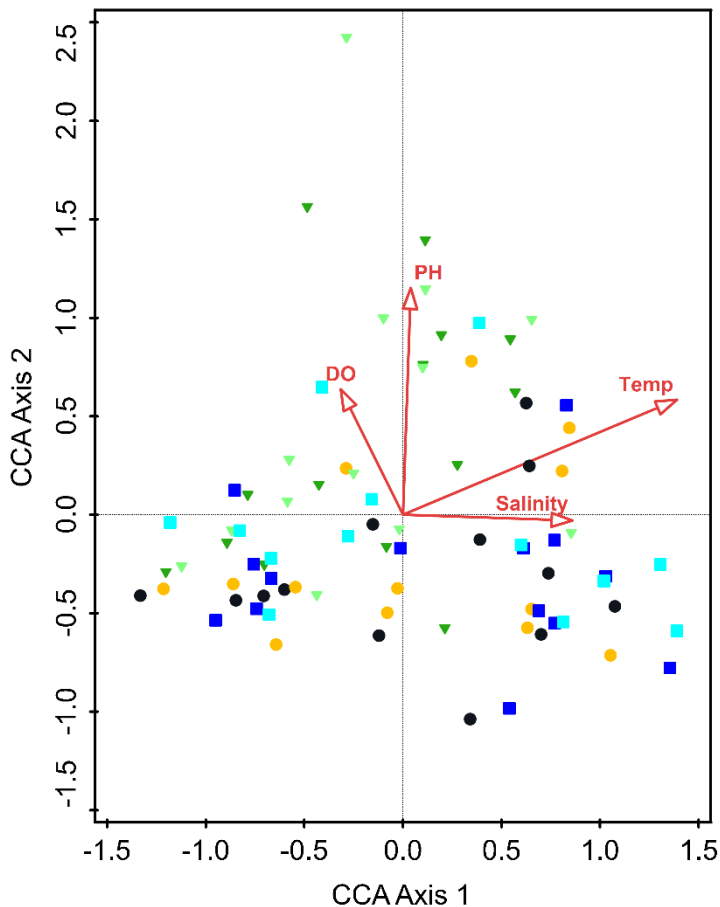
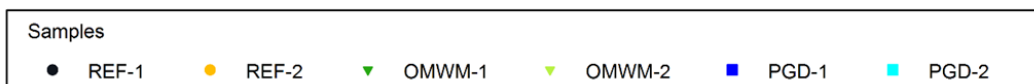


Fig. 7. Sample-Environment biplot derived from canonical correspondence analysis (CCA) in the salt marsh ponds from May 2022 to June 2023. Samples are color-coded by type of pond. Red arrows are environmental variables: water temperature (Temp), salinity, dissolved oxygen (DO), and pH.



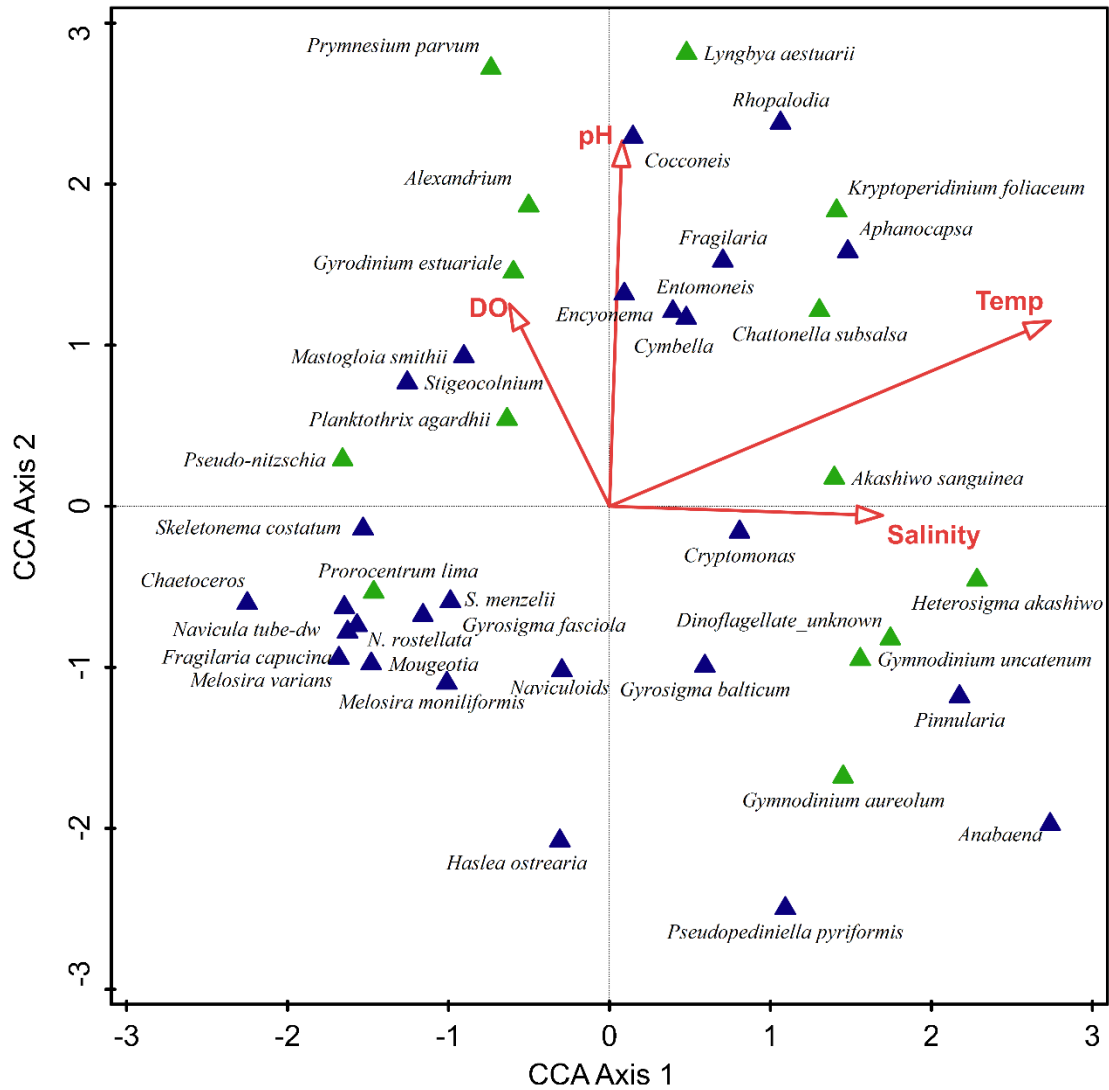


Fig. 8. Species-Environment biplot derived from canonical correspondence analysis (CCA) in salt marsh ponds from May 2022 to June 2023, showing the first 30 taxa with highest weight. Red arrows are environmental variables: water temperature (Temp), salinity, dissolved oxygen (DO), and pH. Symbols in green are HAB species.

DNA-based analysis on algal composition and HAB species from August 2022-June 2023

16S rRNA analysis

Ribosomal Database Project (RDP) analysis based on 16S rRNA sequencing showed that bacteria dominance in the pond microbial community belongs to the major groups of Proteobacteria and Bacteroidetes. However, the sequences of chloroplasts/cyanobacteria that represent autotrophs accounted for as high as 27% of the community in November in OMWM-1 (Fig. 9). Further analyses of BLASTn were performed on the chloroplasts/cyanobacteria sequences against PhytoREF database and revealed the major microalgae groups including chlorophytes (green algae), cyanobacteria (blue-green algae), bacillariophytes (diatoms), haptophytes, and raphidophytes. In addition, several less common groups such as euglenophytes, cryptophytes, chrysophytes, dictyochophytes, eustigmatophytes, and pelagophytes, were identified and lumped into ‘other microalgae’ in Fig. 10.

Cyanobacteria made up most of the chloroplast/cyanobacteria sequences, particularly in warm months (June-August) in REF-2, OMWM-1 and OMWM-2, accounting for as high as 95% of the total abundance. In cool months, e.g., November, December and February, cyanobacteria still accounted for as high as 53% to 87% in OMWM ponds and REF-2 (Fig. 10).

18S rDNA analysis

Sequencing analysis based on 18S rDNA primer set, euk-A7F and euk-570R, showed that microalgae accounted for as high as 91% of eukaryotes, varying with ponds and months (Fig. 11). Results further showed that microalgae communities were composed of diatoms, green algae, haptophytes, and raphidophytes, as well as ‘other’ groups: euglenophytes, cryptophytes, chrysophytes, dictyochophytes, eustigmatophytes, and pelagophytes, consistent with those from the 16S rRNA-based analysis. Furthermore, the 18S-based analysis showed dinoflagellates were one of the main components of microalgal communities in these ponds.

DNA-based classifications of HAB species

Significant differences were found between the ability of 16S and 18S analyses to distinguish HAB species. The 16S-based analysis was able to classify cyanobacterial species, while the 18S-based analysis was able to distinguish dinoflagellate harmful species. Most harmful species were consistent with microscopic observations at genus/species level (Table A2 and A4). Both 16S and 18S DNA-based analyses were able to identify raphidophyte harmful species. The 16S-based analysis was able to find *F. japonica* and *H. akashiwo*, while the 18S-based classifications identified a couple more species including *Chattonella subsalsa*, *Chloromorium toxicum*, and *Olisthodiscus luteus*. The 16S-based analysis, on the other hand, showed higher resolution in the classification of harmful species in the group of haptophytes, distinguishing three genera containing potentially harmful species, *Chrysochromulina*, *Prymnesium* and *Phaeocystis* while 18S did not find them

The classifications of the other microalgal groups were comparable between the 16S-based and 18S-based analyses, including diatoms, green algae, cryptophytes, euglenophytes, eustigmatophytes, and pelagophytes.

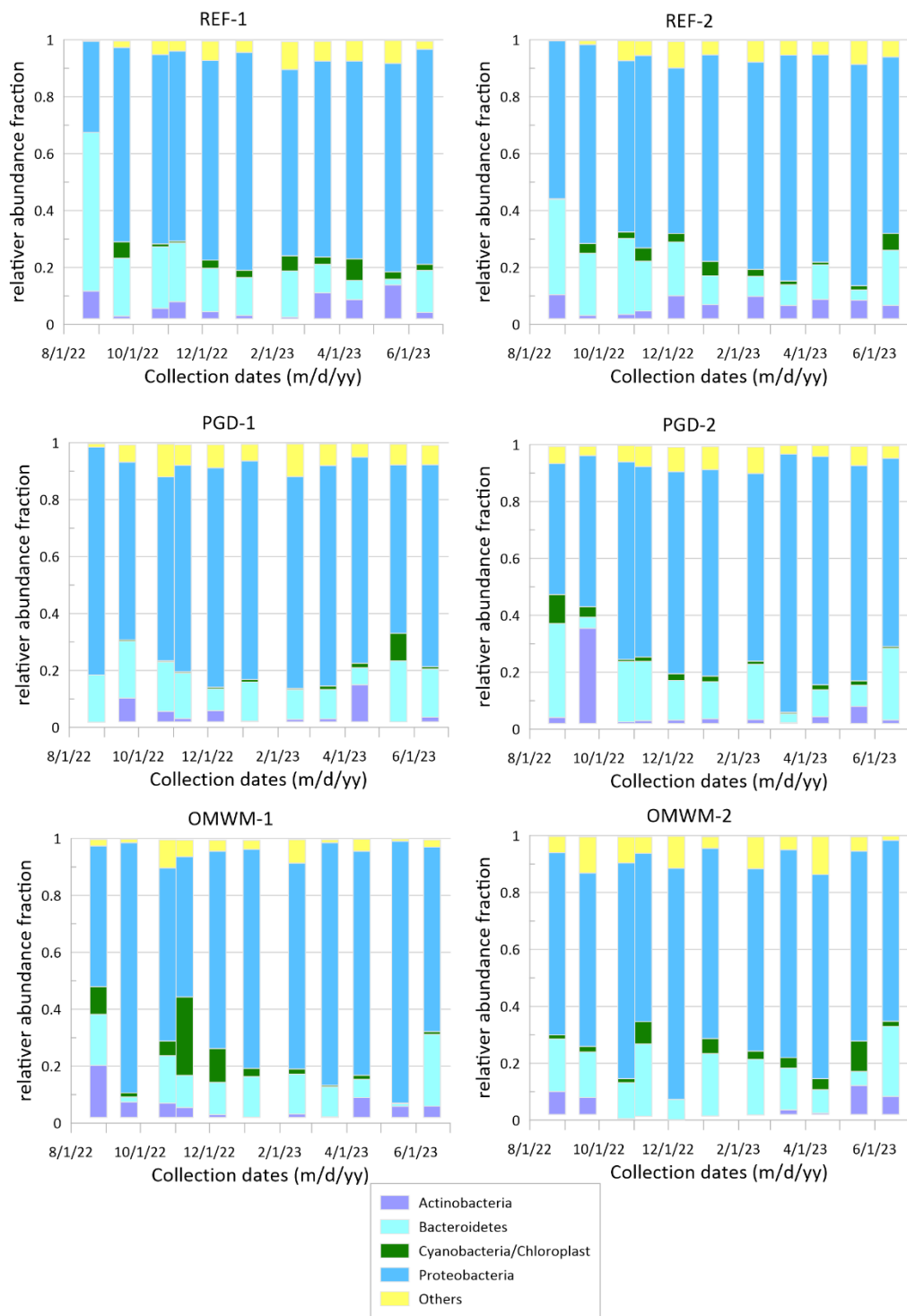


Fig. 9. Compositions of major components of prokaryotes in the salt marsh ponds, derived from the 16S rRNA sequencing. “Other” comprises eukaryote groups.

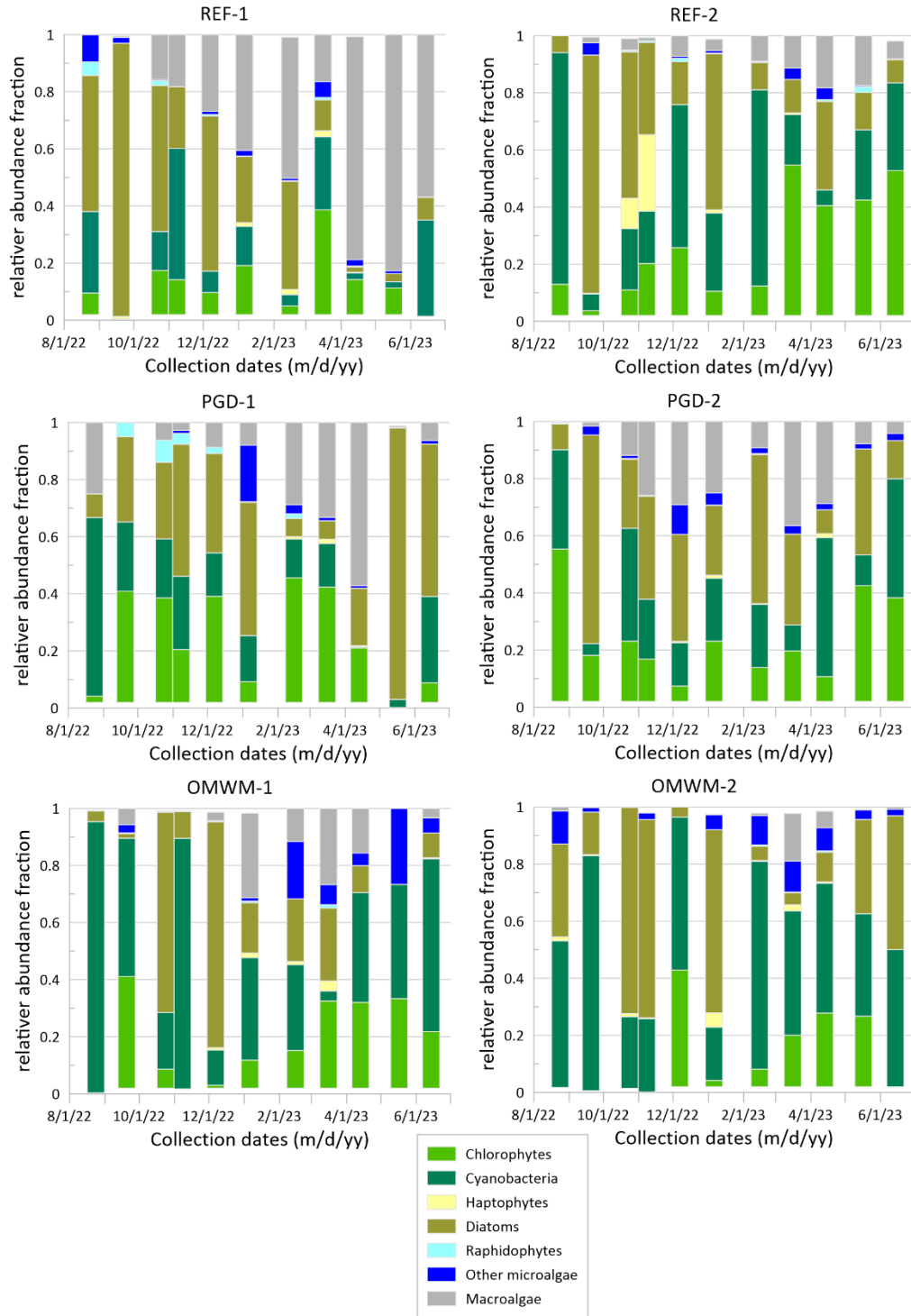


Fig. 10. Compositions of major autotrophic algal groups in salt marsh ponds, derived from the 16S rRNA sequencing.

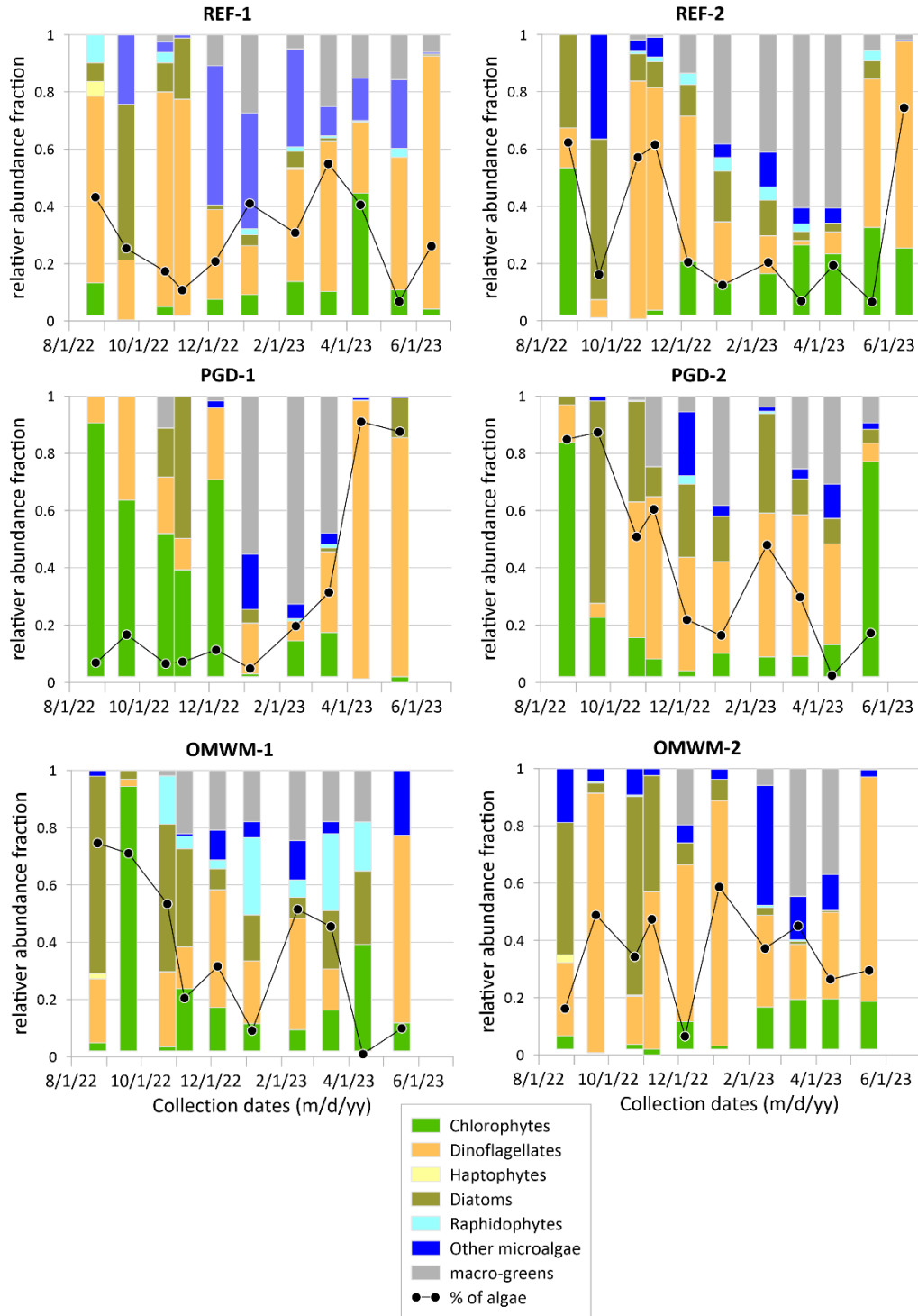


Fig. 11. 18S rDNA-based microalgal community compositions and their percentage (%) in eukaryotes in the salt marsh ponds. The major algal groups are indicated in legend. Other microalgae include: Cryptophytes, Euglenophytes, Chrysophytes, Dictyochophytes, Eustigmatophytes Olisthodiscophytes, Pelagophytes, Phaeophytes, and Rhodophytes.

Spatial and temporal variations of DNA-based algal composition

The DNA-based microalgal community compositions were compared among the ponds for May and August (warm months) as well as for December-January (cold months). Spatial differences between ponds were common in each month and unrelated to the pond type of segment (Fig. 12). PGD-1 differed from the other ponds in both August and December/January, as well as OMWM-2 in December /January and to a lesser degree REF-1 in May. With the exception of PGD-1 and OMWM-2, the other ponds showed considerable similarity in the cold months. whereas in warm months, the ponds showed higher variation in the microalgal community.

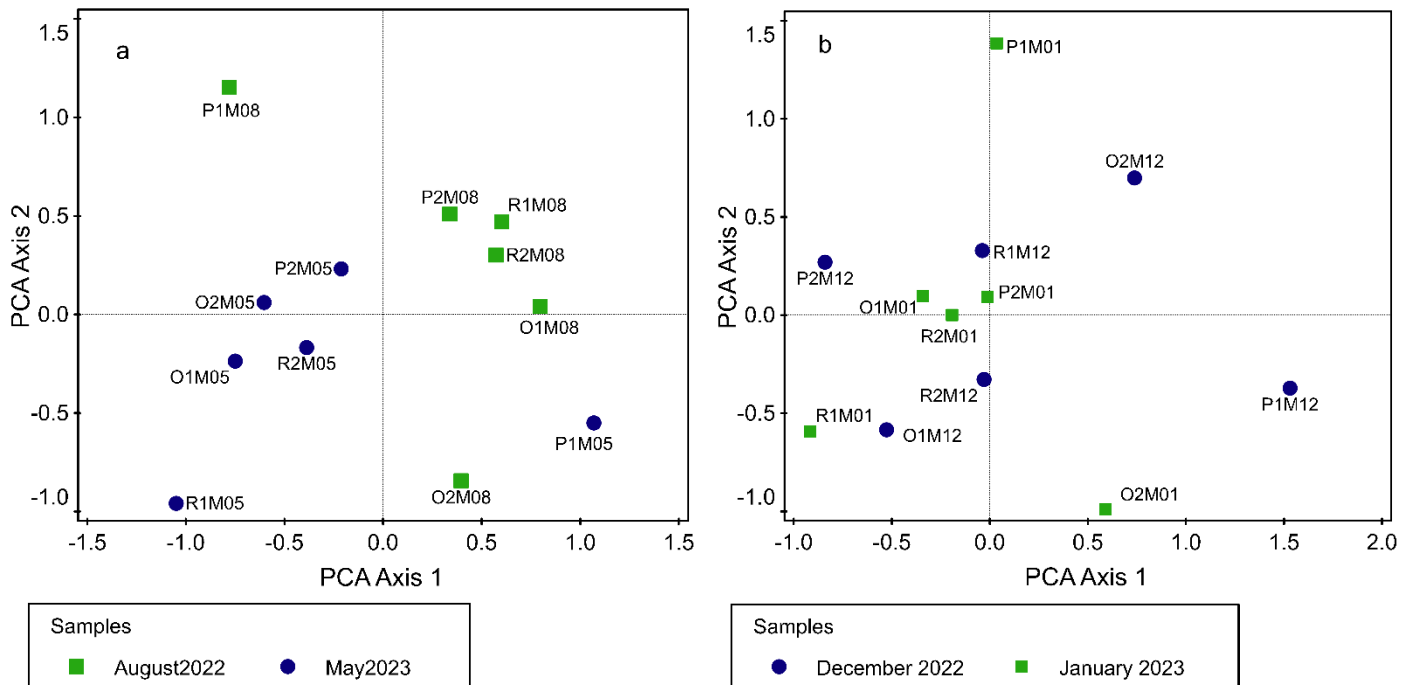


Fig. 12. Spatial and temporal variations of algal compositions based on 18S rDNA sequencing. a: May and August (Aug); b: December and January. Sample labels are composed of ponds+layer+month. Ponds: R-REF, P-PGD, and O-OMWM; layer: M-mix, and months: 05-May and 08-August.

Planktonic (surface) vs. mixed microalgal communities

A few sampling events were performed in November-December 2022 and April-May 2023 on both surface water layer and the mixed samples that included some sediment from the bottom of the pond. The purpose of these two types of sampling was to investigate if the two sampling methods would result in different microalgal compositions especially with regard to HAB abundances. Both microscopic and 18S rDNA-based results showed that microalgal communities collected from the surface water were to a certain extent different from the mixed samples. The microscopic-based analysis was done on species/genus composition and showed more

differences between the two types of samples. This is indicated by the distance between the two types of samples in the NMDS ordination diagrams (Fig. 13, b).

The composition of genera obtained through 18S rDNA-based analysis, showed a higher distinction between the surface water and mixed samples in REF-2 April (R2S04 -R2M04), PGD-1 December (P1S12-P1M12), and REF-2 November (R2S11-R2M11) (Fig. 13a).

Microscopy-based analysis showed distinctive differences between surface and mixed samples in PGD-1 April (P1S04-P1M04), REF-1 November (R1S11-R1M11), and OMWM-2 May (O2S05-O2M05) (Fig. 13b).

Both microscopy and 18S rDNA-based classifications showed that in November and December the mixed samples from REF-2 and PGD-1 were dominated by dinoflagellates, while the surface water had abundant diatoms in both ponds. In REF-2, surface water and mixed microalgal communities were comparable in April, however, the mixed sample had more abundant filamentous green algae. The May OMWM-2 surface water sample had abundant harmful *P. parvum* in the microscopic observation, but green algae, particularly *Picochlorum*, appeared abundant in DNA-based classification. It is worth noting that both methods revealed that the species diversity in mixed samples, as numbers of classified species, was generally higher than that of surface samples. These results suggest that mixed microalgal sampling that includes both water and some sediment from the bottom of the pond would perform better than only collecting surface water for the identification of HAB presence in SMPs, regardless of whether the analyses are performed by microscopy or DNA.

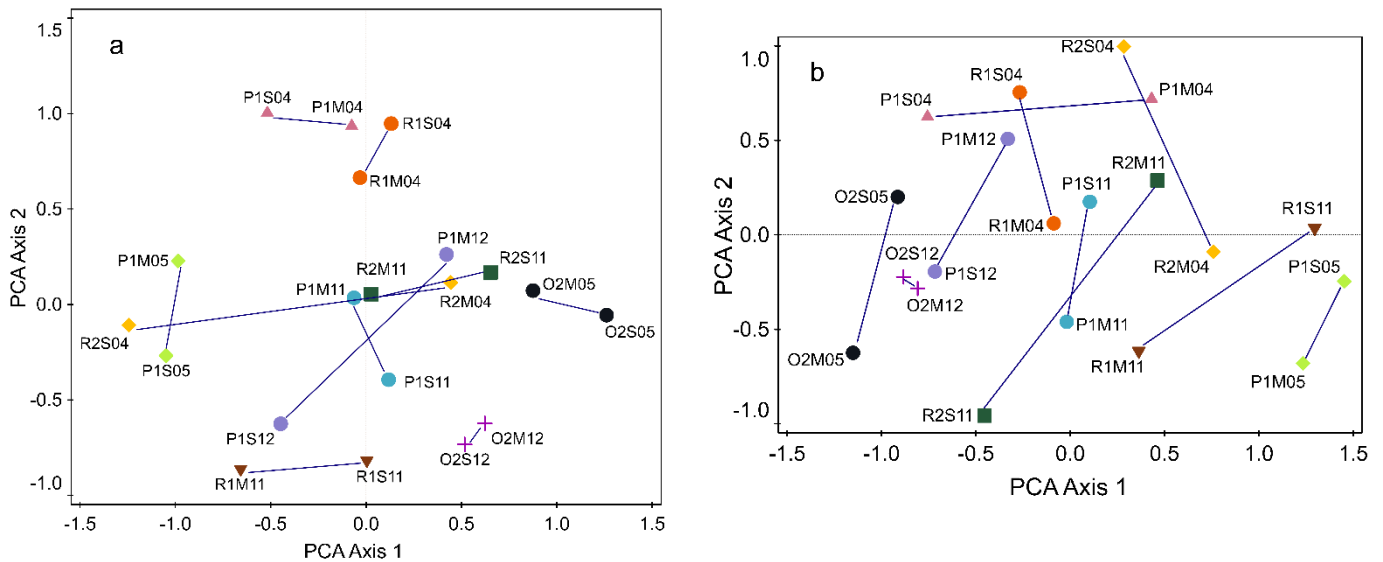


Fig. 13. Comparison of microalgal composition between surface and mixed samples collected in April-May 2023 and November-December 2022. a: based on 18S rDNA sequencing; b: based on microscopic counts. Sample labels are composed of ponds+layer+month. Ponds: R-REF, P-PGD, and O-OMWM; Layers: S-surface and M-mix; Months: MM.

Detection of harmful algae and biotoxins from July and August 2023 sampling events

Environmental parameters from July and August 2023

All six SMPs were sampled for detection of biotoxins on July 28, August 11 and 30th. Measurements of water parameters are plotted in Fig. 14. Salinity ranged between 28-33 ppt in most SMPs. OMWM-2 exhibited higher salinity compared to other ponds and the highest salinity was 36 ppt on August 30. The water temperature decreased by ~ 5°C from July to August. Spatially, the YSI-measured water temperature showed a general trend of increase from REF to OMWM, and to PGD ponds. The pH measurements varied mostly between 7 and 8. The highest pH was detected in OMWM sites around 9 from the July 28 and August 11 sampling events. Specific conductivity was highly correlated with salinity ($R^2 = 0.98$). Dissolved oxygen (DO) concentration varied from time to time and pond to pond. Extreme low DO of 0.1 mg/l was detected in REF-2 on July 28, and near hypoxic (2.4 mg/l) in PGD-2. DO saturation was closely related to DO concentration ($R^2 = 0.91$).

Variations of microalgal composition from July and August 2023

Microalgal species composition and cell density (in cells/mL) are presented in Table A3. In total, 18 samples were analyzed, collected from each of the six SMPs on 7/28, 8/11, and 8/30 in 2023. Many harmful and potentially toxic algae were detected in the samples, including dinoflagellates *A. sanguinea*, *K. foliaceum*, *A. carterae*, *P. lima*, and *Karlodinium* spp., raphidophytes *Ch. subsalsa*, haptophytes *P. parvum* and *H. akashiwo*, and cyanobacteria *L. aestuarii*, *Ph. autumnale* *P. agardhii*. Most HAB species were dominant, with high cell density > 10⁴ cells/mL.

The NMDS analysis based on the species cell density showed temporal and spatial patterns from July to August 2023 among the ponds (Fig. 15). In each pond, algal community composition varied between the three sampling events. The difference in algal species composition between July and late August was higher than that between mid- and late August for most ponds. The management history of the marsh (PGD, OMWM, or Ref) did not seem to be a driving factor in the differences in algal communities among ponds. The differences in microalgal composition between two ponds with the same management history was sometimes larger than those between the ponds with different management histories. For instance, PGD-2 and OMWM-2 showed more similarity in the July 28 and August 30 sampling events, in comparison to that between PGD-1 and PGD-2, and between OMWM-1 and OMWM-2 (Fig. 15). This suggests that the variation in HABs species composition and abundance is not related to the management history of the ponds, but rather dependent of in situ conditions present in each pond. These differences were observed despite the similarities in ponds' morphological features and sometimes proximity to each other.

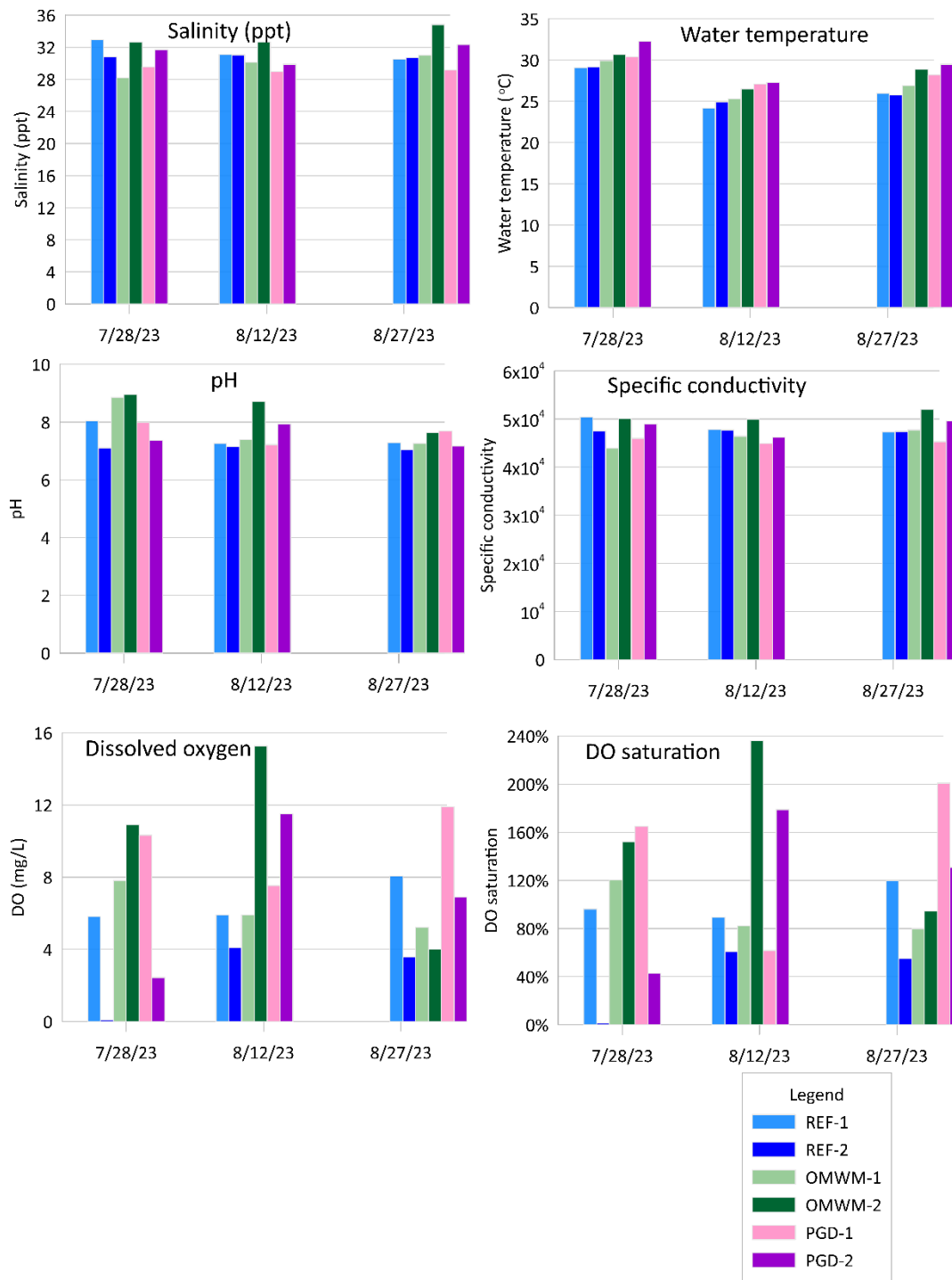


Fig. 14. Measurements of water temperature, salinity, pH, specific conductivity, dissolved oxygen (DO), and DO saturation in July-August 2023 in the salt marsh ponds, Sheepshead Meadow peninsula in Tuckerton, NJ.

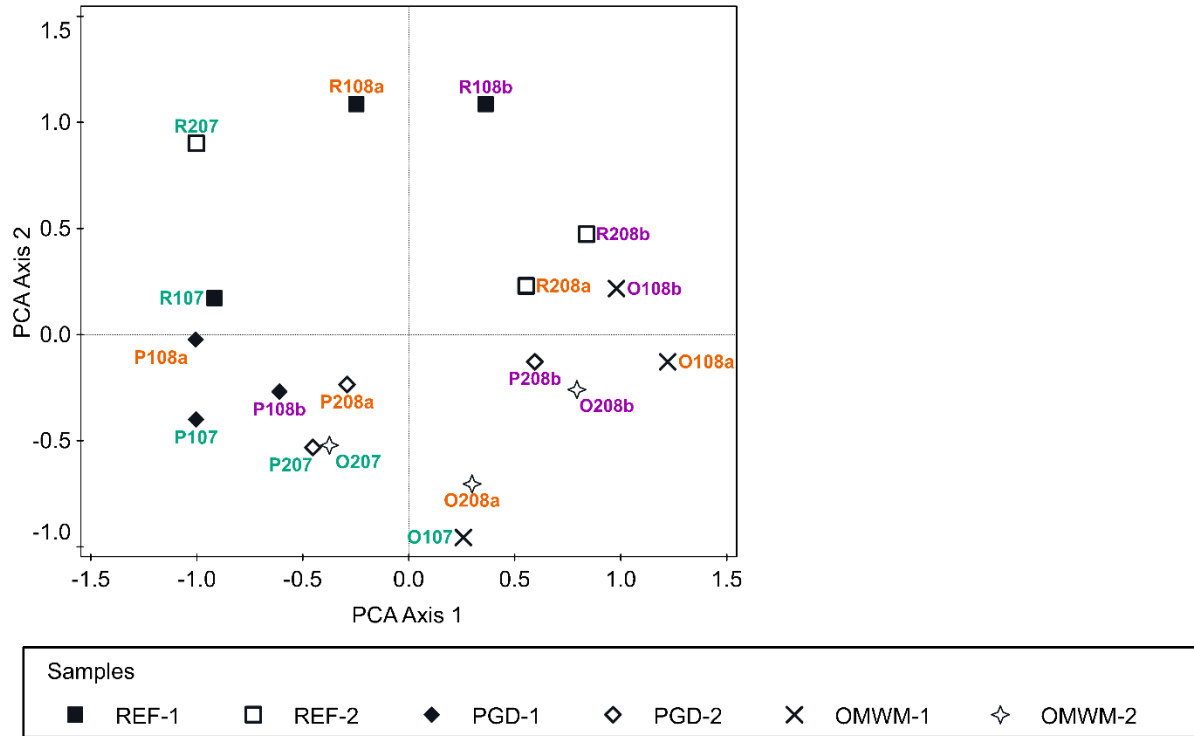


Fig. 15. Comparison of microalgal community among the salt marsh ponds (SMPs) from July to August 2023 based on non-metric multidimensional scaling. SMPs are in different symbols. Each sample is color-coded by month/date. Every sample is labeled with the codes of site (initial letter with 1 or 2), collection month (MM, the 3rd and 4th digits). The samplings on August 11th and 30th are labeled as ‘a’ and ‘b,’ respectively. The scaling is based on sample scores, and the distance between the samples approximates the dissimilarity/similarity of algal communities, measured by the Euclidean distance.

Changes of microalgal composition in relation to environmental variables from July and August 2023 sampling events

Changes in microalgal composition in relation to environmental variables were explored using CCA analysis. Canonical correspondence analysis (CCA) was carried out based on the changes in taxa compositions collected on July 28th, August 11th, and 30th. Water temperature, DO, and salinity were the major (of the examined) factors explaining changes in taxa composition ($p < 0.01$), followed by pH, as shown by CCA analysis (Fig. 17). These four parameters explained about 27% of the total variation of the algal community.

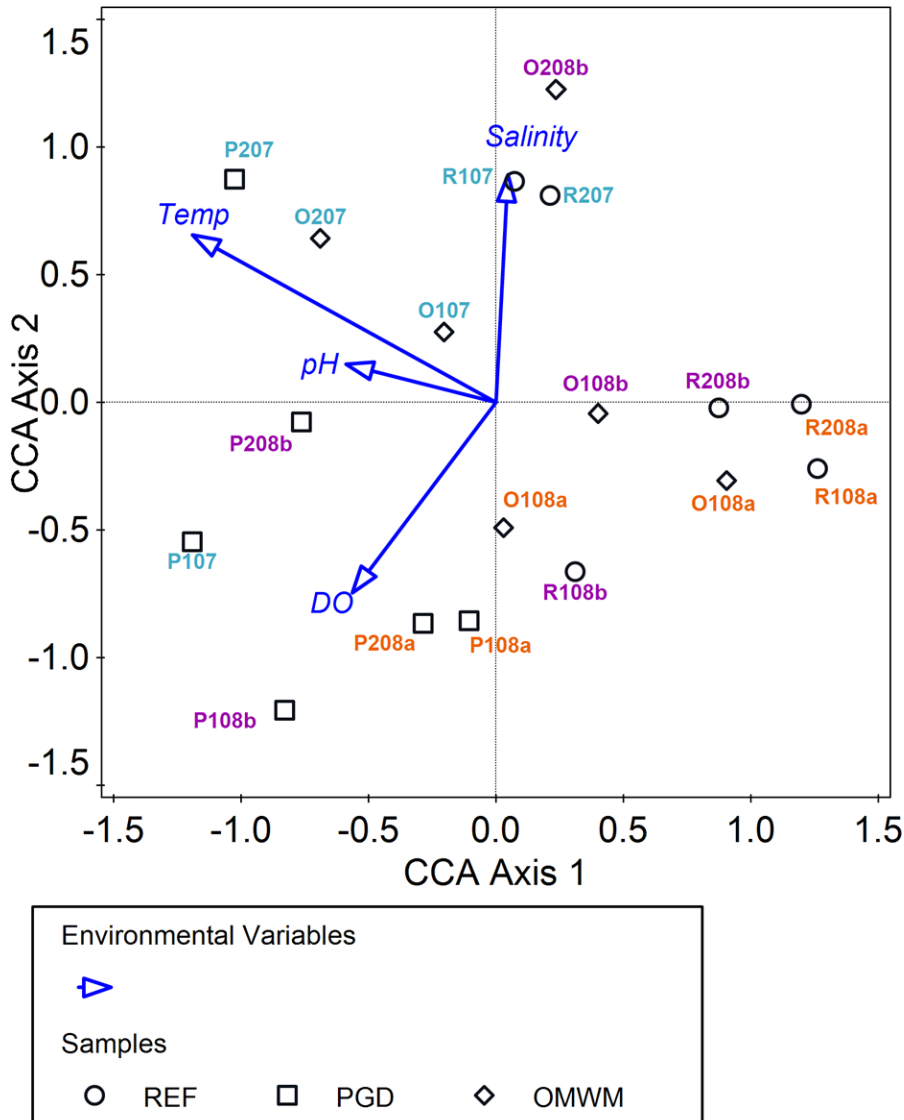


Fig. 16. Sample-Environment biplot derived from constrained Canonical Correspondence Analysis based on microalgal community compositions collected in July and August 2023. Each sampling event is color-coded. Every sample is labeled as salt marsh pond (SMP) site (first 2 codes), collection month (MM, the 3rd and 4th digits), in addition, August 11th and 30th samplings are labeled as ‘a’ and ‘b’, respectively. Temp: water temperature; DO: dissolved oxygen concentration (mg/L).

Algal biotoxins detected from July and August 2023 sampling events

Five algal toxins were detected in the SMPs, including brevetoxin, saxitoxin, okadaic acid, microcystins, and cylindrospermopsins. Furthermore, the results showed multiple toxins were present simultaneously in over half of the samples. Okadaic acid (OA), however, was detected only in OMWM-2, and its concentration reached > 270 µg/L at the end of July (7/28/2023) sampling (Table 4).

Table 4: Results of HAB derived biotoxins in the SMP samples collected from 5/17/2023, 7/28/2023, 8/11/2023, and 8/30/2023. nd: not detected. LOD: limit of detection

Sample ID	Site ID	Collection date	Volume (ml)	Brevetoxin (µg/L)	Saxitoxin (µg/L)	Okadaic acid (µg/L)	Microcystins (µg/L)	Cylindrospermopsin (µg/L)
SMP0167	REF-1	7/28/2023	120	0.43	0.53	nd	nd	nd
SMP0169	REF-2	7/28/2023	150	nd	0.32	nd	nd	nd
SMP0171	PGD-1	7/28/2023	100	nd	0.33	nd	nd	0.37
SMP0173	PGD-2	7/28/2023	90	nd	nd	nd	0.63	5.89
SMP0175	OMWM-1	7/28/2023	100	nd	0.61	nd	0.78	0.76
SMP0177	OMWM-2	7/28/2023	70	2.03	0.91	273.60	nd	2.16
SMP0180	REF-1	8/11/2023	50	nd	0.71	nd	nd	nd
SMP0182	REF-2	8/11/2023	50	nd	4.49	nd	nd	nd
SMP0184	PGD-1	8/11/2023	130	nd	nd	nd	nd	nd
SMP0186	PGD-2	8/11/2023	50	nd	1.91	nd	0.90	0.50
SMP0188	OMWM-1	8/11/2023	50	1.42	0.58	nd	10.60	nd
SMP0190	OMWM-2	8/11/2023	50	nd	nd	15.70	nd	0.80
SMP0192	REF-1	8/30/2023	80	nd	1.27	nd	nd	nd
SMP0196	PGD-1	8/30/2023	90	nd	nd	nd	nd	0.44
SMP0198	PGD-2	8/30/2023	90	nd	4.62	nd	2.13	6.89
SMP0200	OMWM-1	8/30/2023	80	1.10	0.68	nd	nd	0.41
SMP0202	OMWM-2	8/30/2023	80	nd	0.43	43.69	nd	22.13
SMP0151	OMWM-1	5/17/2023	70	nd	2.78	nd	nd	nd

* Method limit of detection (LOD): Brevetoxin: 0.1 µg/L; Saxitoxin: 0.03 µg/L; Okadaic acid: 0.2 µg/L; Microcystins: 0.05 µg/L; Cylindrospermopsin: 0.05 µg/L

Webpage development

A user-friendly website has been constructed to share the harmful algal diversity in the Tuckerton peninsula salt marsh ponds found in this study. The website offers easy access to information about various algal species that were detected in the ponds, including their identification, distribution, morphology, and toxicity. By incorporating multimedia elements of videos and photos, the website aims to reach a broad audience, from researchers to nature enthusiasts. A total of 49 images and 21 videos illustrating 13 HAB species were included on this webpage. Additionally, there is documentation on morphology, ecology, toxicity, distribution, and occurrence for each HAB species. The webpage is accessible to the general public <https://dep.nj.gov/dsr/nj-smp-hab-reservoirs/>.

Discussion

Dynamics of harmful algal blooms in SMPs

Our investigation revealed the presence and dominant role of HABs in intertidal salt marsh ponds, for the first time, on the Tuckerton peninsula. The extent and intensity of the presence of HABs in the study SMPs are remarkable. Spatially and temporally, the distribution of HABs was extensive across all the ponds in the three areas of marshes under different management regimes in summer (June-August) and occasionally in the spring, from March to May. Moreover, HAB species were detected in a few winter sampling events and were dominant in some ponds, such as PGD-2 and OMWM-2. HABs were characterized by extremely high abundance and dominance of one or two HAB species in one pond, e.g., REF-1, PGD-1 and 2, and OMWM-1 and 2, as shown in Appendices Plate A2. However, all the ponds, over the entire study period, displayed highly diverse HAB communities, including dinoflagellates, raphidophytes, haptophytes, and cyanobacteria species. Most HAB species are planktonic; however, benthic species were commonly present and became abundant at times, such as *Amphidinium caterae* (Baig et al. 2006), *Phormidium autumnale* (Harland et al. 2013), and *Lyngbya aestuarii* (Kothari, 2013). All are typical coastal and marine HAB species (Lassus et al. 2016, Steidinger and Castillo, 2018) and possess features that are competitively advantageous (Granéli et al. 2008, Anderson et al. 2021, Medić et al. 2022). For example, many dinoflagellates have a life stage of resting cysts, which serves as a survival strategy under unfavorable conditions (Burkholder et al. 2006, Bravo and Figueroa 2014).

Coastal phytoplankton composition and HAB dynamics are closely regulated by temperature and salinity as well as other physical, chemical, and biological parameters, such as nutrients, potentially leading to HAB proliferation (Cloern, 1996, Anderson et al. 2008, Gobler, 2020). The highly dynamic spatial and temporal variations of HABs in the SMPs are remarkable, since all sampled ponds share similar characteristics in terms of size, depth, and isolation and appear independent of management history.

Temperature is a major driver for the seasonality of phytoplankton community changes (Trombetta et al. 2019). Summer temperature is generally about 5 °C higher in the Sheepshead Meadows peninsula ponds than that in the surrounding Barnegat Bay and Little Egg Harbor (Ren, 2013, 2015) owing to the semi-isolation and small water bodies which are totally exposed under direct sunlight. For the same reasons, winter temperature is warmer in the ponds than the surrounding tidal creeks (Smith and Able, 1994), where the differences generally range between 8-12 °C, therefore making SMPs ideal winter refugia for a variety of fishes, as well as winter algal growth and blooms when it is sunny and calm. The impact of temperature was observed in the study SMPs with HAB species *Ch. subsalasa*, *K. foliaceum*, *G. uncatenatum*, and *A. sanguinea* occurring at higher temperatures, while *Pseudo-nitzschia* and *P. lima* preferring lower temperatures. A bloom of harmful dinoflagellate *P. lima* was observed in OMWM-2 in December. A positive correlation between temperature and pH was found for the 2023 July and August three sampling events. The relationship between water pH and temperature is often mediated by phytoplankton photosynthesis (Raven et al. 2020). A positive relationship between

pH and temperature indicates an increase in phytoplankton photosynthesis, associated with algal growth and biomass, following rising temperature.

The salinity gradient among the study ponds is a function of pond location, tides, weather and precipitation, and human activities. The study area is connected to the Atlantic Ocean via the Little Egg Inlet, with a tidal range of ~1 meter. REF ponds, located in the south near the inlet, showed less fluctuations in salinity compared to the other ponds. PGD ponds, especially PGD-1, located farther from the ocean, are simultaneously affected by freshwater discharges from the residential areas. A positive correlation between salinity and temperature, as found in the study SMPs, indicates a strong effect of weather-associated water evaporation on salinity in the ponds. A heat wave in August 2022 resulted in an elevation of salinity in most ponds. Salinity reached 45 ppt in OMWM-2, which was extremely high compared to the other ponds but not unprecedented in this area (see Able et al. 2005).

The dissolved oxygen (DO) level generally indicates the metabolism of a pond, resulting from competing photosynthesis, respiration, surface-atmosphere exchange, and reduction/oxidation of sediments. The DO concentration in the ponds was generally above 5 mg/L in the late morning to early afternoon sampling, and oversaturation of oxygen was detected during afternoon sampling in spring and summer. Hypoxia, defined as $DO \leq 2$ mg/L, was detected in REF-1 in April 2023 when the sampling started around 8 o'clock in the morning, and the DO concentration was < 5 mg/L in all the other ponds, suggesting hypoxic conditions in the SMPs at night alleviated by photosynthesis of macro- and micro- algae with the increasing light intensity and temperature into late morning. In addition, two more incidents of near-hypoxia, with DO ~2.6 mg/L, were detected in PGD-1 in May and in REF-2 in September, suggesting more consumption of oxygen in these ponds compared to the other ponds on the same dates. The fluctuations of oxygen hyper-saturation and hypoxia in the salt marsh pools are consistent with findings in previous studies (Spivak et al. 2017, Koop-Jakobsen and Gutbrod 2019).

The above-mentioned four environmental parameters, temperature, salinity, pH, and DO explain a small portion of microalgal community variance among the ponds, including HAB species (Fig. 9). Other factors that were not measured in this study, such as eutrophication, nutrient stoichiometry and ratios, organic matter, and presence and abundance of grazers, etc., are known to contribute to the proliferation of HABs (Glibert and Burkholder, 2018, Wurtsbaugh et al. 2019). In addition, sediment type and benthic communities can play significant roles in the biogeochemistry of these shallow and small ponds.

HABs and biotoxins

Our study revealed, for the first time in this area, the presence of diverse algal biotoxins in the salt marsh ponds. It is common for the same HAB species to produce diverse types of toxins, and a toxin can be associated with a variety of toxin-producing algae (Wang 2008). Our study showed that multiple HAB species were abundant across the studied SMPs (Table A3). It is difficult, at this point, to associate the types of toxins with specific HAB species, or vice versa, due to the complexity of the HAB species-toxin production relationships and limited data points from this study. Nevertheless, this study demonstrated some correlations between the toxins and

HAB species. For instance, Okadaic acid (OA) was detected in (and only in) OMWM-2. The highest OA concentration ($> 270 \mu\text{g/L}$), detected on 7/30/2023, was coincident with a high cell density of *P. lima* (1.6×10^4 cells/mL) and *P. minimum* (6.5×10^3 cells/mL). OA was detected in OMWM-2 on 8/30/2023 but one magnitude lower than that in July, corresponding to a much lower cell density of *P. lima* and *P. minimum*. The results are consistent with a previous study showing that *Prorocentrum* species are one of the major OA producers (Moreira-González et al. 2022). Interestingly, the same cell density of *P. lima* and *P. minimum* was detected in OMWM-1 on 8/11/2023 and 8/30/2023; however, OA was not detected in these samples.

Low concentrations of Brevetoxin were detected with highest in OMWM-2 on 7/28/2023 at $2.03 \mu\text{g/L}$, and lower concentrations in REF-1 in July and OMWM-1 in both August samplings (Table 4). *Ch. subsalsa* and *H. akashiwo*, both HAB species associated with brown or red tide blooms and known to produce Brevetoxin (Zhang et al. 2006) were found in the same sampling sites with low abundances (Table A3). The only previous detection of Brevetoxin was reported by the New Jersey DEP Bureau of Marine Water Monitoring (BMWM) in very low concentrations of 0.04-0.1 ppb after a bloom event with *Karenia* spp. occurring of the Atlantic coast in 2022 (NJ BMWM personal communication).

Two types of cyanotoxins, Microcystins and Cylindrospermopsins, were detected in the SMPs. The presence of cyanotoxins corresponded with cyanobacteria cell counts in most samples. However, in a few other samples, there did not seem to be a correlation between cyanotoxin presence and cell counts. For example, cyanotoxins were detected in PGD-2 on 7/28/2023, OMWM-2 on 8/11/2023, and PGD-1 on 8/30/2023, but no cyanobacteria cells were encountered during microscopy examinations (Table A3). A higher concentration of Microcystins was detected in OMWM-1 on 8/11/2023 at $10.6 \mu\text{g/L}$; however, there was not much difference in the cell counts of cyanobacteria between OMWM-1 and other ponds (Table A3). Unfortunately, due to funding constraints, DNA-based analysis was not performed, and we were not able to verify if cyanobacteria species presence was detectable or not in these samples.

The de-coupling of toxin presence and harmful algae detection may be caused by different reasons. Methodologically, when a sample is dominated by a particular group (e.g., Dinoflagellates or Haptophytes) and cyanobacteria are present but at much lower density, it is possible that cyanobacteria may not be encountered before the total cell counts reach the stopping point of the method. On the other hand, toxins can attach to organic and inorganic particles; thus, even if the cells are dead or dissolved, toxins can remain in the system and be detectable. Moreover, toxin production can vary with different strains of the same HAB species, as well as the physiological and environmental conditions of the cells (Ismael et al. 1999, Accoroni et al. 2018). Studies also showed that the production of toxins can be associated with the stage of a HAB event (Accoroni et al. 2017). More studies are needed to provide further insight into the presence of toxins and HABs in salt marsh ponds because of their importance to ecology and environment, economics, and human health of coastal communities.

Planktonic and mixed algal community

Planktonic samples, which were collected from the upper 10 cm of the pond water, represented only the phytoplankton present in the ponds, whereas the mixed samples would contain

phytoplankton, periphytic and epiphytic algae, and benthic microalgae due to the shallowness of the ponds and light penetration. The diversity of microalgae in the mixed samples was generally higher than in the phytoplankton samples. In fall and winter, phytoplankton was sparse and composed of diatoms, whereas diverse communities were observed in mixed samples associated to soil, organic clumps or plants. It is worth noting that *P. lima*, which was dominant in the mixed sample of OMWM-2 in December, is epibenthic (Alvarez et al. 2022). In spring and summer, however, phytoplankton was often predominantly composed of HAB species with flagella, including diverse dinoflagellates, haptophyte *P. parvum* and raphidophyte *Ch. Subsalsa*. However, in the mixed samples, there was often an increased presence of epiphytic/periphytic diatoms. These results demonstrated the diversity of algae distribution within the ponds despite the relative homogeneity in physical and chemical conditions. This needs to be carefully taken into consideration when it comes to monitoring HABs and biotoxins.

DNA-based and morphology-based classifications on HAB species

Microscopic algae, as a vital component of aquatic systems, are a diverse and polyphyletic group encompassing organisms from widely different taxonomic domains, including eukaryotes and prokaryotes. HABs consist of diverse species from diatoms, dinoflagellates, raphidophytes, haptophytes, and cyanobacteria.

Microscope analysis remains the primary method in microscopic algae analysis. In this study, the use of microscopy provided more detailed information in the identification and enumeration of algal compositions and HAB species than the DNA-based methods, with some exceptions. However, microscope analysis is highly dependent on the level of expertise and experience of the analysts. The method has limitations, especially when it comes to very small and morphologically similar species with features difficult to distinguish under light microscopy. Furthermore, many soft-body algae can appear different morphologically because of their life stages and/or angles they're viewed through the microscope lens. These can be challenging even for well-trained analysts.

The combination of 16S rRNA based and 18S rDNA metabarcoding, as this study shows, provided information on photosynthetic cyanobacteria and eukaryotic phytoplankton, its community diversity and composition, as well as the relative abundance of major taxonomic groups. Some challenges in the metabarcoding of microscopic algae and HAB species are 1) the need for adequate PCR primers that can simultaneously prioritize the sequencing of highly informative regions (Hugerth et al. 2014) and 2) the need for comprehensive DNA barcode reference libraries that can provide reliable biodiversity and taxonomic information for a wide range of aquatic samples (Weigand et al. 2019). As shown in this and other studies (e.g., Bennke et al. 2018), the 16S-based analysis could not be used to detect dinoflagellates. The amplification of the 16S rRNA genes of dinoflagellate plastids is much more difficult compared to other eukaryotic algae as the genomes of dinoflagellate plastids can undergo unusual processes making their metagenomic identification difficult. The lack of dinoflagellate identification can also be attributed to the underrepresentation of dinoflagellate reference barcodes in the PhytoREF database (0.5% of all entries). The 18S rDNA gene marker has been used to identify eukaryote groups of microorganisms. Compared to 16S marker, 18S-based barcoding showed higher

resolution in classification on most microalgal groups, especially dinoflagellate HABs. However, the method cannot provide information on cyanobacteria species. It is recommended that microscopy observations be supplemented with DNA-based analysis using gene markers when investigating and monitoring HABs, depending on the HAB species found in the water body through microscopy.

Summary

This study showed, for the first time, the extensive presence of HABs in SMPs in coastal NJ marshes. It demonstrated that SMPs can serve as natural microcosms providing niche conditions, environmentally and ecologically, for the growth and dominance of certain HAB species. The shallow and semi-enclosed water bodies are ideal for biomass accumulation, especially under calm and sunny weather when algal growth can be stimulated under optimum temperature and light conditions. This explains the abundance and low diversity of HABs in a specific pond despite the overall high diversity of HABs across all the ponds. Further studies leading to more in-depth comprehension of the conditions and factors driving species-specific HABs and algal toxins in the ponds, as well as their effects on fish and shellfish, are needed.

The study results supported our hypothesis that the tidal SMPs, forming unique microhabitats, can serve as reservoirs of HAB species. The HAB species were found across all pond management types. Many toxin-producing species have been previously detected along the New Jersey Coast (Mahoney et al. 1989, Gastrich, 2000) and in Barnegat Bay-Little Egg Harbor (Olsen and Mahoney 2001, Ren, 2013, Ren et al. 2017), but not in the salt marsh ponds, and never to this extent in terms of species diversity, cell density, and temporal and spatial coverages. These SMPs are subject to frequent tides and floodings during which the HAB species are transported, providing the potential for HAB developments to the coastal open waters.

Outreach

The established website can serve as a resource for the general public and students K-12 or higher on HABs in NJ coastal marshes. It also serves as an interface to connect with NJ communities and inform them of the presence of HABs in these ponds and the potential for toxins presence. In addition, our outreach activities included 1) a poster presentation at the Atlantic Estuary Research Society (AERS) spring 2023 meeting; 2) an article published in the Coastodian newsletter: <https://njseagrant.org/wp-content/uploads/2023/04/Coastodian-Winter-2023-1.pdf>; 3) a poster presentation at the 2023 National Estuarine Research Reserve Association (NERRA/NERRS) annual meeting; and 4) a manuscript was submitted to the journal Regional Studies in Marine Science. Access link: https://papers.ssrn.com/sol3/papers.cfm?abstract_id=4935264.

Recommendations

This study demonstrated, for the first time, that HABs contribute to the dynamics of SMPs in the New Jersey coastal marshes and the presence of HAB-derived toxins in SMPs regardless of their

management history (i.e., unaltered, PGD, or OMWM). This finding has significant implications for wetland ecology and environmental and human health. It shows that the study of HABs can play an important role in qualifying and quantifying coastal marsh functions and habitat conditions. Consequently, a long-term assessment of the changing climate impacts on HAB dynamics in NJ and other states along the Mid-Atlantic seaboard would be necessary. The detected HAB producing toxins in this study are known to be associated with fish kills and sublethal effects on fish foraging and predation avoidance, as well as fish survival and fish recruitment (Reis Costa 2016). Research studies have also revealed an array of adverse effects of algal toxins on birds, from reduced feeding activity, inability to lay eggs, and loss of motor coordination to death (Shumway et al. 2003, Trotter et al. 2022). Furthermore, those toxins may cause serious human health issues through the consumption of contaminated fish and shellfish and/or direct contact with the waters containing toxic HABs. Meanwhile, increasing evidence has shown that algae-derived toxins in water can be aerosolized into the air, posing adverse health issues to humans and animals through inhalation (Plaas and Pearl 2021, Acker et al. 2021). Therefore, follow-up studies on the quantification of biotoxin production and trophic transfer of the toxins in these ponds may be necessary, given the ecological and health impact of the HABs and HAB-derived biotoxins.

Our findings suggest that additional metrics associated with the NJ SMPs, such as algal compositions and biotoxins, have the potential to be added to the existing indicators and tools used at present for assessing wetland biotic integrity and developing water quality standards. Salt marshes function as filters to remove nutrients, pollutants, and organic wastes from coastal waters (Tiner 1985). The mechanisms of algae species succession and the proliferation of HABs in SMPs have not been studied. Retaining the filtered nutrients may have led to the formation and sustaining of HABs in the studied marsh ponds, as numerous studies have shown the correlations between nutrient inputs and HABs in estuarine and coastal ecosystems. For this reason, the assessment of the functions and habitat conditions of coastal marsh is recommended to be refined, taking into consideration the HABs and biotoxins in the salt marsh ponds.

This study showed that the microscopy examination provides more holistic information on algal community composition, including HABs, compared to either 16S- or 18S rDNA based analysis. It is recommended that the microscopy method be supplemented with DNA-based analysis in monitoring HABs in the coastal ecosystems.

Based upon the findings of this study, monitoring of HAB presence and toxin levels in the New Jersey salt marsh ponds would be strongly recommended to protect the coastal ecosystems from the potential harmful effects of these HABs. Also, coastal communities need to be informed of the HAB presence and potential toxicity related to the HAB presence, especially during the warm season when highest HAB abundances have been detected.

The predicted climate change, with higher temperatures and sea level rise, could heighten, through increased marsh flooding, the potential for more frequent HAB inoculation as SMPs are increasingly flooded and connected to estuarine open waters and their fisheries. This study shows that it is increasingly important to integrate SMPs into the assessment of wetland conditions and functions and their effect on both land cover and coastal water effects. Our project findings

provided insights into SMPs' function as reservoirs of HABs and HAB derived toxins. These findings are important for other coastal states because they reveal the need to consider and monitor for the potential HAB presence. This would be an important step to prepare management strategies for protecting coastal ecosystems resources and ensuring environmental justice for disadvantaged communities while facing increasing challenges from future climate changes.

References

1. Able, K. W., Smith, K. J., & Hagan, S. M. (2005). Fish composition and abundance in New Jersey salt marsh pools: Sampling technique effects. *Northeastern Naturalist*, *12*, 485–502. [https://doi.org/10.1656/1092-6194\(2005\)012\[0485:FCAAIN\]2.0.CO;2](https://doi.org/10.1656/1092-6194(2005)012[0485:FCAAIN]2.0.CO;2)
2. Adamowicz, S., & Roman, C. (2005). New England salt marsh pools: A quantitative analysis of geomorphic and geographic features. *Wetlands*, *25*, 279–288.
3. Accoroni, S., Tartaglione, L., Iacovo, E. D., Pichierri, S., Marini, M., Campanelli, A., Dell'Aversano, C., & Totti, C. (2017). Influence of environmental factors on the toxin production of *Ostreopsis cf. ovata* during bloom events. *Marine Pollution Bulletin*, *123*, 262–268. <https://doi.org/10.1016/j.marpolbul.2017.08.049>
4. Accoroni, S., Ceci, M., Tartaglione, L., Romagnoli, T., Campanelli, A., Marini, M., Giuliotti, S., Dell'Aversano, C., & Totti, C. (2018). Role of temperature and nutrients on the growth and toxin production of *Prorocentrum hoffmannianum* (Dinophyceae) from the Florida Keys. *Harmful Algae*, *80*, 140–148. <https://doi.org/10.1016/j.hal.2018.11.005>
5. Anderson, D. M., Burkholder, J. M., Cochlan, W. P., Glibert, P. M., Gobler, C. J., Heil, C. A., Kudela, R., Parsons, M. L., Rensel, J. E. J., Townsend, D. W., Trainer, V. L., & Vargo, G. A. (2008). Harmful algal blooms and eutrophication: Examining linkages from selected coastal regions of the United States. *Harmful Algae*, *8*, 39–53. <https://doi.org/10.1016/j.hal.2008.08.017>
6. Anderson, D. M., Fensin, E., Gobler, C. J., Hoeglund, A. E., Hubbard, K. A., Kulis, D. M., Landsberg, J. H., Lefebvre, K. A., Provoost, P., Richlen, M. L., Smith, J. L., Solow, A. R., & Trainer, V. L. (2021). Marine harmful algal blooms (HABs) in the United States: History, current status, and future trends. *Harmful Algae*, *102*, 101975. <https://doi.org/10.1016/j.hal.2021.101975>
7. Bahls, L. L. (1993). *Periphyton bioassessment methods for Montana streams*. Montana Water Quality Bureau, Department of Health and Environmental Science, Helena, Montana.
8. Baig, H. S., Saifullah, S. M., & Dar, A. (2006). Occurrence and toxicity of *Amphidinium carterae* Hulbert in the North Arabian Sea. *Harmful Algae*, *5*, 133–140. <https://doi.org/10.1016/j.hal.2005.06.010>
9. Bennke, C. M., Pollehne, F., Müller, A., Hansen, R., Kreikemeyer, B., & Labrenz, M. (2018). The distribution of phytoplankton in the Baltic Sea assessed by a prokaryotic 16S rRNA gene primer system. *Journal of Plankton Research*, *40*(3), 244–254. <https://doi.org/10.1093/plankt/fby008>
10. Bravo, I., & Figueroa, R. (2014). Towards an ecological understanding of dinoflagellate cyst functions. *Microorganisms*, *2*, 11–32. <https://doi.org/10.3390/microorganisms2010011>
11. Burkholder, J. M., Azanza, R. V., & Sako, Y. (2006). The ecology of harmful dinoflagellates. In E. Granéli & J. T. Turner (Eds.), *Ecology of harmful algae, ecological studies* (pp. 53–66). Springer. https://doi.org/10.1007/978-3-540-32210-8_5
12. Campbell, A. D., Fatoyinbo, L., Goldberg, L., & Lagomasino, D. (2022). Global hotspots of salt marsh change and carbon emissions. *Nature*, *612*, 701–706. <https://doi.org/10.1038/s41586-022-05355-z>

13. Cloern, J. (1996). Phytoplankton bloom dynamics in coastal ecosystems: A review with some general lessons from sustained investigation of San Francisco Bay, California. *Reviews of Geophysics*, 34. <https://doi.org/10.1029/96RG00986>
14. Cole, J. R., Wang, Q., Fish, J. A., Chai, B., et al. (2013). Ribosomal Database Project: Data and tools for high throughput rRNA analysis. *Nucleic Acids Research*, 42, D633–642.
15. Currin, C. A., Wainright, S. C., Able, K. W., Weinstein, M. P., & Fuller, C. M. (2003). Determination of food web support and trophic position of the mummichog, *Fundulus heteroclitus*, in New Jersey smooth cordgrass (*Spartina alterniflora*), common reed (*Phragmites australis*), and restored salt marshes. *Estuaries*, 26, 495–510.
16. Curry, K. D., Wang, Q., Nute, M. G., et al. (2022). Emu: Species-level microbial community profiling for full-length Nanopore 16S reads. <https://doi.org/10.1101/2021.05.02.442339>
17. Decelle, J., Romac, S., Stern, R. F., Bendif, E. M., Zingone, A., et al. (2015). PhytoREF: A reference database of the plastidial 16S rRNA gene of photosynthetic eukaryotes with curated taxonomy. *Molecular Ecology Resources*, 15, 1435–1445. <https://doi.org/10.1111/1755-0998.12401>
18. Elsey-Quirk, T., Watson, E. B., Raper, K., Kreeger, D., Paudel, B., Haaf, L., Maxwell-Doyle, M., Padeletti, A., Reilly, E., & Velinsky, D. J. (2022). Relationships between ecosystem properties and sea-level rise vulnerability of tidal wetlands of the U.S. Mid-Atlantic. *Environmental Monitoring and Assessment*, 194, 292. <https://doi.org/10.1007/s10661-022-09949-y>
19. Esenkulova, S., Tabata, A., Sutherland, B. J. G., & Haigh, N. (2019). Combining metabarcoding and morphological approaches to identify phytoplankton taxa associated with harmful algal blooms. <https://doi.org/10.1101/816926>
20. Fernandes, L. F., et al. (2014). Diversity and toxicity of the diatom *Pseudo-nitzschia* Peragallo in the Gulf of Maine, Northwestern Atlantic Ocean. *Deep Sea Research Part II: Topical Studies in Oceanography*, 103, 139–162. <https://doi.org/10.1016/j.dsr2.2013.06.022>
21. Gastrich, M. D. (2000). Harmful algal blooms in coastal waters of New Jersey. 44.
22. Gillevet, P., Sikaroodi, M., et al. (2010). Quantitative assessment of the human gut microbiome using multitag pyrosequencing. *Chemistry & Biodiversity*, 7(5), 1065–1075.
23. Glibert, P. M., & Burkholder, J. M. (2018). Causes of harmful algal blooms. In S. E. Shumway, J. M. Burkholder, & S. L. Morton (Eds.), *Harmful algal blooms* (pp. 1–38). Wiley. <https://doi.org/10.1002/9781118994672.ch1>
24. Gobler, C. J. (2020). Climate change and harmful algal blooms: Insights and perspective. *Harmful Algae*, 91, 101731. <https://doi.org/10.1016/j.hal.2019.101731>
25. Guillou, L., Bachar, D., Audic, S., et al. (2012). The Protist Ribosomal Reference database (PR2): A catalog of unicellular eukaryote small sub-unit rRNA sequences with curated taxonomy. *Nucleic Acids Research*, 41, D597–D604. <https://doi.org/10.1093/nar/gks1160>
26. Granéli, E., Weberg, M., & Salomon, P. S. (2008). Harmful algal blooms of allelopathic microalgal species: The role of eutrophication. *Harmful Algae*, 8, 94–102. <https://doi.org/10.1016/j.hal.2008.08.011>

27. Greenberg, R., Maldonado, J. E., Droege, S., & McDonald, M. V. (2006). Tidal marshes: A global perspective on the evolution and conservation of their terrestrial vertebrates. *BioScience*, 56, 675. [https://doi.org/10.1641/0006-3568\(2006\)56\[675:TMAGPO\]2.0.CO;2](https://doi.org/10.1641/0006-3568(2006)56[675:TMAGPO]2.0.CO;2)
28. Harland, F., Wood, S., Moltchanova, E., et al. (2013). *Phormidium autumnale* growth and anatoxin-a production under iron and copper stress. *Toxins*, 5, 2504–2521. <https://doi.org/10.3390/toxins5122504>
29. Hugerth, L. W., Muller, E. E. L., Hu, Y. O. O., Lebrun, L. A. M., Roume, H., Lundin, D., Wilmes, P., & Andersson, A. F. (2014). Systematic design of 18S rRNA gene primers for determining eukaryotic diversity in microbial consortia. *PLoS ONE*, 9, e95567. <https://doi.org/10.1371/journal.pone.0095567>
30. Ibelings, B. W., Kurmayer, R., Azevedo, S. M. F. O., Wood, S. A., Chorus, I., & Welker, M. (2021). Understanding the occurrence of cyanobacteria and cyanotoxins. In *Toxic cyanobacteria in water: A guide to their public health consequences, monitoring and management* (2nd ed.). CRC Press.
31. Ismael, A. A.-H., Halim, Y., & Khalil, A.-G. (1999). Optimum growth conditions for *Amphidinium carterae* Hulbert from eutrophic waters in Alexandria (Egypt) and its toxicity to the brine shrimp *Artemia salina*. *Grana*, 38, 179–185. <https://doi.org/10.1080/00173139908559226>
32. James-Pirri, M.-J., Ginsberg, H. S., Erwin, R. M., & Taylor, J. (2009). Effects of open marsh water management on numbers of larval salt marsh mosquitoes. *Journal of Medical Entomology*, 46, 1392–1399. <https://doi.org/10.1603/033.046.0620>
33. Kennish, M. J. (2001). Coastal salt marsh systems in the U.S.: A review of anthropogenic impacts. *Journal of Coastal Research*, 17, 731–748.
34. Kennish, M. J., Meixler, M. S., Petruzzelli, G., & Fertig, B. (2014). Tuckerton Peninsula salt marsh system: A sentinel site for assessing climate change effects. <https://doi.org/10.7282/T3348NBS>
35. Kerkhof, L. J., Dillon, K. P., Häggblom, M. M., & McGuinness, L. R. (2017). Profiling bacterial communities by MinION sequencing of ribosomal operons. *Microbiome*, 5, 116. <https://doi.org/10.1186/s40168-017-0336-9>
36. King, J. R., & Jackson, D. A. (1999). Variable selection in large environmental data sets using principal components analysis. 11.
37. Kirwan, M. L., & Mudd, S. M. (2012). Response of salt-marsh carbon accumulation to climate change. *Nature*, 489, 550–553. <https://doi.org/10.1038/nature11440>
38. Koop-Jakobsen, K., & Gutbrod, M. S. (2019). Shallow salt marsh tidal ponds—An environment with extreme oxygen dynamics. *Frontiers in Environmental Science*. <https://doi.org/10.3389/fenvs.2019.00137>
39. Kothari, A. (2013). Comparative genomic analyses of the cyanobacterium, *Lyngbya aestuarii* BL J, a powerful hydrogen producer. *Frontiers in Microbiology*. <https://doi.org/10.3389/fmicb.2013.00363>

40. Lassus, P. (Ed.). (2016). *Toxic and harmful microalgae of the world ocean*. International Society for the Study of Harmful Algae-ISSHA; United Nations Educational, Scientific and Cultural Organisation, Copenhagen; Paris.
41. Lathrop, R. G., Cole, M. B., & Showalter, R. D. (2000). Quantifying the habitat structure and spatial pattern of New Jersey (U.S.A.) salt marshes under different management regimes. *Wetlands Ecology and Management*, 8, 163–172.
42. Laughrey, Z. R., Christensen, V. G., Dusek, R. J., Senegal, S., Lankton, J. S., Ziegler, T. A., Jones, L. C., Jones, D. K., Williams, B. M., Gordon, S., Clyde, G. A., Emery, E. B., & Loftin, K. A. (2022). A review of algal toxin exposures on reserved federal lands and among trust species in the United States. *Critical Reviews in Environmental Science and Technology*, 52, 4284–4307. <https://doi.org/10.1080/10643389.2021.2010511>
43. LeGresley, M., & McDermott, G. (2010). Counting chamber methods for quantitative phytoplankton analysis-Haemocytometer, Palmer-Maloney cell, and Sedgewick-Rafter cell. *Intergovernmental Oceanographic Commission of UNESCO Manual*, 55. UNESCO, Paris, 25-30pp.
44. MacKenzie, R., & Dionne, M. (2008). Habitat heterogeneity: Importance of salt marsh pools and high marsh surfaces to fish production in two Gulf of Maine salt marshes. *Marine Ecology Progress Series*, 368, 217–230. <https://doi.org/10.3354/meps07560>
45. Mahoney, J. B., Olsen, P., & Cohn, M. (1989). Blooms of a dinoflagellate *Gyrodinium cf. aureolum* in New Jersey coastal waters and their occurrence and effects worldwide. *Journal of Coastal Research*, 6, 121–135.
46. Medić, N., Varga, E., de Waal, D. B. V., Larsen, T. O., & Hansen, P. J. (2022). The coupling between irradiance, growth, photosynthesis, and prymnesin cell quota and production in two strains of the bloom-forming haptophyte, *Prymnesium parvum*. *Harmful Algae*, 112, 102173. <https://doi.org/10.1016/j.hal.2022.102173>
47. Meixler, M. S., Kennish, M. J., & Crowley, K. F. (2018). Assessment of plant community characteristics in natural and human-altered coastal marsh ecosystems. *Estuaries and Coasts*, 41, 52–64. <https://doi.org/10.1007/s12237-017-0296-0>
48. Moreira-González, A. R., Rosa, K. M. S., & Mafra, L. L. (2021). Prevalence of okadaic acid in benthic organisms associated *Prorocentrum lima* complex in a sub-tropical estuary. *Food Additives & Contaminants: Part A*, 39(2), 382–396. <https://doi.org/10.1080/19440049.2021.1992512>
49. Narayan, S., Beck, M. W., Wilson, P., Thomas, C. J., Guerrero, A., Shepard, C. C., Reguero, B. G., Franco, G., Ingram, J. C., & Trespalacios, D. (2017). The value of coastal wetlands for flood damage reduction in the Northeastern USA. *Scientific Reports*, 7, 9463. <https://doi.org/10.1038/s41598-017-09269-z>
50. Nowruzzi, B., & Porzani, S. J. (2021). Toxic compounds produced by cyanobacteria belonging to several species of the order Nostocales: A review. *Journal of Applied Toxicology*, 41, 510–548. <https://doi.org/10.1002/jat.4088>
51. Olsen, P. S., & Mahoney, J. B. (2001). Phytoplankton in the Barnegat Bay–Little Egg Harbor estuarine system: Species composition and picoplankton bloom development. In M. J. Kennish

- (Ed.), *Characterization of Barnegat Bay – Little Egg Harbor, New Jersey, estuarine system and watershed assessment. Journal of Coastal Research, Special Issue No. 32*, 115–143.
52. Plaas, H. E., & Paerl, H. W. (2021). Toxic cyanobacteria: A growing threat to water and air quality. *Environmental Science & Technology*, 55, 44–64. <https://doi.org/10.1021/acs.est.0c06653>
 53. Potapova, M., Markarian, D., King, A., & Ayccock, L. (2024). Microbial eukaryotes in natural and artificial salt marsh pools. *Coasts*, 4, 287–305. <https://doi.org/10.3390/coasts4020015>
 54. Raven, J. A., Gobler, C. J., & Hansen, P. J. (2020). Dynamic CO₂ and pH levels in coastal, estuarine, and inland waters: Theoretical and observed effects on harmful algal blooms. *Harmful Algae*, 91, 101594. <https://doi.org/10.1016/j.hal.2019.03.012>
 55. Reis Costa, P. (2016). Impact and effects of paralytic shellfish poisoning toxins derived from harmful algal blooms to marine fish. *Fish and Fisheries*, 17, 226–248. <https://doi.org/10.1111/faf.12105>
 56. Ren, L. (2013). *Project technical report to NJDEP*. <http://nj.gov/dep/dsr/barnegat/finalreport-year1/phytoplankton-year1.pdf>
 57. Ren, L., Belton, T. J., Schuster, R., & Enache, M. (2017). Phytoplankton index of biotic integrity and reference communities for Barnegat Bay–Little Egg Harbor, New Jersey: A pilot study. *Journal of Coastal Research*, 78, 89–105. <https://doi.org/10.2112/SI78-009.1>
 58. Rey, J. R., Walton, W. E., Wolfe, R. J., et al. (2012). North American wetlands and mosquito control. *International Journal of Environmental Research and Public Health*, 9, 4537–4605. <https://doi.org/10.3390/ijerph9124537>
 59. Rochlin, I., James-Pirri, M.-J., Adamowicz, S. C., Wolfe, R. J., Capotosto, P., Dempsey, M. E., Iwanejko, T., & Ninivaggi, D. V. (2012). Integrated marsh management (IMM): A new perspective on mosquito control and best management practices for salt marsh restoration. *Wetlands Ecology and Management*, 14.
 60. Rogers, K., Kelleway, J. J., Saintilan, N., Megonigal, J. P., Adams, J. B., Holmquist, J. R., Lu, M., Schile-Beers, L., Zawadzki, A., Mazumder, D., & Woodroffe, C. D. (2019). Wetland carbon storage controlled by millennial-scale variation in relative sea-level rise. *Nature*, 567, 91–95. <https://doi.org/10.1038/s41586-019-0951-7>
 61. Sharma, L. L., Aery, N. C., Kumar, A., & Gupta, M. C. (2016). Diatoms as component of fish diet in natural aquatic environment 2.
 62. Shumway, S. E., Allen, S. M., & Dee Boersma, P. (2003). Marine birds and harmful algal blooms: Sporadic victims or under-reported events? *Harmful Algae*, 2, 1–17. [https://doi.org/10.1016/S1568-9883\(03\)00002-7](https://doi.org/10.1016/S1568-9883(03)00002-7)
 63. Smith, K. J., & Able, K. W. (1994). Salt-marsh tide pools as winter refuges for the mummichog, *Fundulus heteroclitus*, in New Jersey. *Estuaries*, 17, 226. <https://doi.org/10.2307/1352572>
 64. Spivak, A. C., Gosselin, K., Howard, E., Mariotti, G., Forbrich, I., Stanley, R., & Sylva, S. P. (2017). Shallow ponds are heterogeneous habitats within a temperate salt marsh

- ecosystem. *Journal of Geophysical Research: Biogeosciences*, 122, 1371–1384. <https://doi.org/10.1002/2017JG003780>
65. Steidinger, K. A., & Meave del Castillo, M. E. (Eds.). (2018). *Guide to the identification of harmful microalgae in the Gulf of Mexico, Volume I: Taxonomy*. St. Petersburg, FL, 384 pp. <http://myfwc.com/research/redtide/research/scientific-products/>
 66. Sullivan, M., & Currin, C. (2002). Community structure and functional dynamics of benthic microalgae in salt marshes. pp. 81–106. https://doi.org/10.1007/0-306-47534-0_6
 67. ter Braak, C. J. F., & Šmilauer, P. (2012). *CANOCO reference manual and CanoDraw for Windows. User's guide: Software for canonical community ordination. Version 5.0*. Microcomputer Power, Ithaca, NY, USA.
 68. Tiner, R. W., Jr. (1985). *Wetlands of New Jersey*. U.S. Fish and Wildlife Service, National Wetlands Inventory, Newton Comer, MA. 117 pp.
 69. Tracy, E. J., & South, G. R. (1989). Composition and seasonality of micro-algal mats on a salt marsh in New Brunswick, Canada. *British Phycological Journal*, 24, 285–291. <https://doi.org/10.1080/00071618900650301>
 70. Trainer, V. L., Bates, S. S., Lundholm, N., Thessen, A. E., Cochlan, W. P., Adams, N. G., & Trick, C. G. (2012). *Pseudo-nitzschia* physiological ecology, phylogeny, toxicity, monitoring and impacts on ecosystem health. *Harmful Algae*, 14, 271–300. <https://doi.org/10.1016/j.hal.2011.10.025>
 71. Trombetta, T., Vidussi, F., Mas, S., et al. (2019). Water temperature drives phytoplankton blooms in coastal waters. *PLOS ONE*, 14, e0214933. <https://doi.org/10.1371/journal.pone.0214933>
 72. Trottet, A., George, C., Drillet, G., & Lauro, F. M. (2022). Aquaculture in coastal urbanized areas: A comparative review of the challenges posed by harmful algal blooms. *Critical Reviews in Environmental Science and Technology*, 52, 2888–2929. <https://doi.org/10.1080/10643389.2021.1897372>
 73. U.S. EPA. (2002). *Methods for evaluating wetland condition: Using algae to assess environmental conditions in wetlands*. Office of Water, U.S. Environmental Protection Agency, Washington, DC. EPA-822-R-02-021.
 74. Van Acker, E., Huysman, S., De Rijcke, M., Asselman, J., De Schampelaere, K. A. C., Vanhaecke, L., & Janssen, C. R. (2021). Phycotoxin-enriched sea spray aerosols: Methods, mechanisms, and human exposure. *Environmental Science & Technology*, 55, 6184–6196. <https://doi.org/10.1021/acs.est.1c00995>
 75. Vaulot, D. S., Geisen, F., Mahé, F., & Bass, D. (2022). Pr2-primers: An 18S rRNA primer database for protists. *Molecular Ecology Resources*, 22(1), 168–179.
 76. Wolfe, R., Zarebicki, P., & Meredith, W. (2022). The evolution of saltmarsh mosquito control water management practices relative to coastal resiliency in the Mid-Atlantic and northeastern United States. *Wetlands Ecology and Management*, 30, 1099–1108. <https://doi.org/10.1007/s11273-021-09817-5>

77. Wurtsbaugh, W. A., Paerl, H. W., & Dodds, W. K. (2019). Nutrients, eutrophication and harmful algal blooms along the freshwater to marine continuum. *WIREs Water*, 6, e1373. <https://doi.org/10.1002/wat2.1373>
78. Yoon, T. H., Kang, H. E., Kang, C. K., Lee, S. H., Ahn, D. H., Park, H., & Kim, H. W. (2016). Development of a cost-effective metabarcoding strategy for analysis of the marine phytoplankton community. *PeerJ*, 4, e2115. <https://doi.org/10.7717/peerj.2115>
79. Zedler, J. B. (1980). Algal mat productivity: Comparisons in a salt marsh. *Estuaries*, 3, 122–131. <https://doi.org/10.2307/1351556>
80. Zhang, Y., Fu, F. X., Whereat, E., Coyne, K. J., & Hutchins, D. A. (2006). Bottom-up controls on a mixed-species HAB assemblage: A comparison of sympatric *Chattonella subsalsa* and *Heterosigma akashiwo* (Raphidophyceae) isolates from the Delaware Inland Bays, USA. *Harmful Algae*, 5(3), 310-320.

Appendices

Table A1: Mean values, standard deviation (SD), and coefficient of variation (COV) of replicate measurements of environmental parameters in SMPs, taken during December 2022, February 2023, and June 2023 sampling events.

Table A2: Algal taxa, encountered as ‘common’, ‘abundant’ and ‘highly abundant’ in at least one sample, and their occurrences in SMPs and months. Potential harmful and toxic species are in bold.

Table A3: Algal species and their cell density in the salt marsh ponds (SMPs) samples collected on 7/28/2023, 8/11/2023, and 8/30/2023.

Table A4: Comparison of algal classifications derived from 18S- and 16S-based DNA sequencing.

Plate A1 Light micrographs of major harmful algae from salt marsh ponds between June 2022 to June 2023.

Plate A2 Light micrographs of live samples, showing the dominance of harmful algae in salt marsh ponds, between June 2022 to June 2023.

Table A1: Mean values, standard deviation (SD), and coefficient of variation (COV) of replicate measurements of environmental parameters in SMPs, taken during December 2022, February 2023, and June 2023 sampling events.

SMPs	Date		Salinity (ppt)	Temp (°C)	Specific Conductivity	pH	DO (mg/L)	DO sat. (%)
REF-1	Dec 2022	Mean	30.60	10.57	47247.33	7.63	8.16	89.10%
		SD	0.06	0.16	61.78	0.02	0.70	6.60%
		COV	0.19%	1.47%	0.13%	0.32%	8.58%	7.41%
	Feb 2023	Mean	30.75	7.84	47744.33	7.84	10.97	113.30%
		SD	0.02	0.04	31.56	0.03	0.10	0.53%
		COV	0.08%	0.48%	0.07%	0.40%	0.91%	0.47%
	Jun 2023	Mean	31.49	22.87	48241.33	7.36	6.36	92.00%
		SD	0.00	0.04	4.44	0.00	0.03	1.13%
		COV	0.01%	0.19%	0.01%	0.06%	0.49%	1.23%
REF-2	Dec 2022	Mean	29.74	10.40	46090.00	7.55	7.83	85.00%
		SD	0.16	0.33	226.67	0.00	0.62	5.33%
		COV	0.55%	3.21%	0.49%	0.06%	7.92%	6.27%
	Feb 2023	Mean	29.38	7.90	45798.33	7.77	10.31	104.93%
		SD	0.04	0.00	40.44	0.00	0.13	1.96%
		COV	0.12%	0.00%	0.09%	0.06%	1.23%	1.86%
	Jun 2023	Mean	30.55	23.00	46954.67	7.38	6.40	92.47%
		SD	0.01	0.00	11.56	0.00	0.14	1.37%
		COV	0.03%	0.00%	0.02%	0.06%	2.12%	1.49%
OMWM-1	Dec 2022	Mean	25.78	10.53	40485.67	7.59	7.83	82.53%
		SD	0.18	0.18	220.44	0.03	0.08	1.11%
		COV	0.70%	1.69%	0.54%	0.41%	1.08%	1.35%
	Feb 2023	Mean	25.35	8.17	40070.00	7.57	9.68	96.87%
		SD	0.00	0.09	7.33	0.01	0.10	0.98%
		COV	0.02%	1.09%	0.02%	0.18%	1.03%	1.01%
	Jun 2023	Mean	30.05	23.33	46293.67	7.98	9.47	135.37%
		SD	0.04	0.18	80.22	0.09	1.28	18.02%
		COV	0.13%	0.76%	0.17%	1.09%	13.49%	13.31%
OMWM-2	Dec 2022	Mean	24.53	11.47	38639.67	7.49	7.45	76.77%
		SD	0.07	0.49	98.44	0.02	0.29	0.96%
		COV	0.30%	4.26%	0.25%	0.24%	3.94%	1.24%
	Feb 2023	Mean	25.72	8.83	40530.00	7.66	10.35	105.87%
		SD	0.01	0.04	30.67	0.00	0.06	0.91%
		COV	0.04%	0.50%	0.08%	0.06%	0.60%	0.86%
	Jun 2023	Mean	32.87	24.07	50182.33	8.75	10.05	163.43%
		SD	0.02	0.42	51.11	0.12	0.87	14.02%
		COV	0.07%	1.75%	0.10%	1.32%	8.69%	8.58%
PGD-1	Dec 2022	Mean	26.57	9.33	41733.33	7.46	7.99	81.63%
		SD	0.13	0.22	187.11	0.03	0.32	2.89%
		COV	0.48	2.38%	0.45%	0.39%	4.06%	3.54%
	Feb 2023	Mean	27.32	8.13	42847.67	7.54	10.04	101.97%
		SD	0.02	0.04	12.44	0.04	0.45	6.09%
		COV	0.06	0.55%	0.03%	0.47%	4.45%	5.97%
	Jun 2023	Mean	28.45	23.07	44056.33	7.28	7.41	107.27%
		SD	0.00	0.04	4.22	0.02	0.20	1.64%
		COV	0.02	0.19%	0.01%	0.24%	2.67%	1.53%
PGD-2	Dec 2022	Mean	27.02	10.00	42278.00	7.51	7.99	83.70%
		SD	0.07	0.20	108.00	0.02	0.06	0.47%
		COV	0.25	2.00%	0.26%	0.27%	0.72%	0.56%
	Feb 2023	Mean	28.81	8.90	44899.67	7.57	9.59	100.30%
		SD	0.01	0.07	34.22	0.00	0.07	0.27%
		COV	0.05	0.75%	0.08%	0.00%	0.76%	0.27%
	Jun 2023	Mean	30.54	24.20	46972.67	7.66	7.49	111.53%
		SD	0.03	0.07	35.78	0.04	0.00	1.42%
		COV	0.09	0.28%	0.08%	0.46%	0.06%	1.28%

Table A2: Algal taxa, encountered as ‘common,’ ‘abundant,’ and ‘highly abundant’ in at least one sample, and their occurrences in SMPs and months. Potential harmful and toxic species are in bold.

Taxon Names	SMP	Months
Diatoms		
<i>Amphora cingulata</i>	REF-1&2, OMWM-1	Feb-Mar, May-Jun,
<i>Caloneis</i> sp.	OMWM-2,	Aug
<i>Campylodiscus</i> sp.	OMWM-1	May
<i>Chaetoceros tenuissimus</i>	PGD-2	Feb
<i>Chaetoceros</i> sp.	OMWM-1	Mar
<i>Cocconeis</i> spp.	REF-1, OMWM-1&2, PGD-2	May, Jun
<i>Cyclotella</i> spp.	PGD-1, OMWM-1	May, Aug
<i>Cylindrotheca closterium</i>	All	Dec-Jan, Apr-Jul
<i>Cymbella</i> sp.	REF-1&2, OMWM-1&2, PGD-1	Jun-Jul, Sept
<i>Entomoneis</i> sp.	REF-2, PGD-1&2, OMWM-1&2	May-Jul, Nov
<i>Fragilaria gracilis</i>	REF-1, OMWM-2	Jun, Sept
<i>Gyrosigma balticum</i>	REF-2, PGD-2, OMWM-1	Feb, May, Aug-Oct,
<i>Gyrosigma fasciola</i>	PGD-1	May
<i>Gyrosigma parkerii</i>	REF-1	Dec
<i>Haslea ostrearia</i>	REF-1	Mar-Apr
<i>Licmophora flabellata</i>	OMWM-2	Apr
<i>Mastogloia smithii</i>	OMWM-2	Nov, Feb, Jun-Jul
<i>Melosira moniliformis</i>	REF-1&2	Jan, May-June,
<i>Melosira varians</i>	PGD-1	Feb
<i>Minidiscus proschkinae</i>	PGD-1&2	Sept
<i>Minutocellus scriptus</i>	PGD-2, OMWM-1&2	Apr, Aug-Sept
<i>Navicula recens</i>	REF-1	May
<i>Navicula veneta</i>	REF-2, PGD-1, OMWM-1&2	Oct, Dec, Jun
<i>Navicula viridula</i>	PGD-1	Sept
<i>Naviculoids</i>	All	Jan-Apr, Jun, Aug, Oct-Dec
<i>Nitzschia palea</i>	OMWM-1&2	Aug, Oct
<i>Nitzschia</i> spp.	OMWM-1, PGD-2	May, Oct-Nov
<i>Pleurosigma</i> sp.	REF-2, PGD-1&2	Jun
<i>Pleurosigma salinarum</i>	REF-1, PGD-1, OMWM-1	May-Jun, Sept, Nov
<i>Proschkinia</i> spp.	PGD-1&2	May-June
<i>Pseudo-nitzschia</i> sp.	REF-1&2, PGD-1, OMWM-1&2	Jan, Dec
<i>Rhopalodia</i> sp.	OMWM-2	July
<i>Skeletonema costatum</i>	PGD-1&2	Jan
<i>Skeletonema menzelii</i>	REF-1, PGD-2	Jan
<i>Striatella unipunctata</i>	OMWM-1	June
<i>Synedra</i> sp.	REF-1	Jan
<i>Surirella costricta</i>	REF-1	May
<i>Navicula, tube-dwelling</i>	REF-2, OMWM-1&2, PGD-1	Dec-Feb, Jun
Dinoflagellates		
<i>Akashiwo sanguinea</i>	PGD-1&2, REF-2	May-Jul
<i>Alexandrium</i> sp.	OMWM-2	June
<i>Amphidinium carterae</i>	PGD-2, OMWM-1	Jan-Feb, July
<i>Gymnodinium aureolum</i>	REF-1, PGD-1&2	Apr, Aug

Table A2 (Continued): Algal taxa, encountered as ‘common’, ‘abundant’ and ‘highly abundant’ in at least one sample, and their occurrences in SMPs and months. Potential harmful and toxic species are in bold.

Taxon_Names	SMP	months
<i>Gyrodinium estuariale</i>	PGD-2	Mar, Nov
<i>Gyrodinium uncatenum</i> <i>(syn. Levanderina fissa)</i>	REF-1, PGD-1&2, OMWM-2	Jun-Aug
<i>Kryptoperidinium foliaceum</i>	PGD-1&2, OMWM2	Jun-Jul
<i>Prorocentrum lima</i>	REF-2, OMWM-1&2	Nov-Dec, Jan, Mar-Jun, Aug-Sept
<i>Heterocapsa niei</i>	PGD-2	Aug
<i>Oxyrrhis marina</i>	OMWM-1&2, PGD-1&2	Jun, Sept
Cyanobacteria		
<i>Merismopedia</i> sp.	OMWM-2	Aug
<i>Lyngbya aestuarii</i> <i>(or L. majuscula)</i>	OMWM-1&2	June-Aug
<i>Phormidium autumnale</i>	OMWM-2	Feb
<i>Planktothrix agardhii</i>	REF-1&2, OMWM-1&2, PGD-2	Nov, Jan, April, Jun
<i>Aphanocapsa</i> sp.	OMWM-2,	Aug
<i>Chroococcus</i> sp.	OMWM-1	Sept
<i>Spirulina</i> sp.	REF-2	May
Chlorophytes		
<i>Golenkinia radiata</i>	PGD-1	Sept
<i>Pandorina</i> sp.	PGD1&2, OMWM-1	Mar, May, Sept
<i>Stigeocolnium</i> sp.	REF-1&2, OMWM-1&2	Jan, Apr, Jun
<i>Pyramimonas virginica</i>	OMWM-2	Aug
<i>Mougeotia</i> sp.	REF-1, PGD-1	Jan-Feb
<i>Pyramimonas</i> sp.	PGD-1	Jan
Cryptophytes		
<i>Cryptomonas</i> sp.	OMWM-1&2, PGD-1&2	Jun, Sept
Raphidophytes		
<i>Heterosigma akashiwo</i>	REF-1, PGD-1&2	Jul-Aug
<i>Chattonella subsalsa</i>	REF-2, PGD-2, OMWM-2	Jun- Aug
Haptophytes		
<i>Hymenomonas carterae</i>	OMWM-1	Dec
<i>Prymnesium parvum</i>	REF-1&2, OMWM-1&2	Apr-May, Jun

Table A3: Algal species and their cell density in the salt marsh ponds (SMPs) samples collected on 7/28/2023, 8/11/2023, and 8/30/2023.

Sample Info	Taxa	Cell density (cells/mL)
SMP00167	<i>Levanderina fissa</i>	23984
REF-1	<i>Kryptoperidinium foliaceum</i>	6124
7/28/2023	<i>Chattonella subsalsa</i>	255
	<i>Akashiwo sanguinea</i>	1021
	diatoms (pennates)	255
SMP00169	<i>Kryptoperidinium foliaceum</i>	1429
REF-2	microzooplankton	3266
7/28/2023	<i>Mesodinium rubrum</i>	408
	<i>Eutreptiella</i> sp.	204
SMP00171	<i>Kryptoperidinium foliaceum</i>	58917
PGD-1	<i>Heterosigma akashiwo</i>	14845
7/28/2023	<i>Prymnesium parvum</i>	17629
	small Naviculoid	464
	<i>Entomoneis paludosa</i>	464
SMP00173	<i>Kryptoperidinium foliaceum</i>	2807
PGD-2	<i>Prymnesium parvum</i>	6889
7/28/2023	<i>Heterosigma akashiwo</i>	3827
	<i>Chattonella subsalsa</i>	8420
	<i>Karlodinium veneficum</i>	4082
	<i>Levanderina fissa</i>	1276
	<i>Cylindrotheca closterium</i>	510
	<i>Minutocellus scriptus</i>	255
SMP00175	<i>Chattonella subsalsa</i>	12860
OMWM-1	<i>Alexandrium</i> sp.	5920
7/28/2023	small Naviculoids	612
	<i>Karlodinium veneficum</i>	612
	<i>Prorocentrum lima</i>	408
	<i>Heterocaspa niei</i>	408
	<i>Pleurosigma salinarum</i>	204
	<i>Levanderina fissa</i>	612
	<i>Lyngbya aestuarii</i> (filament)	204
SMP00177	<i>Prorocentrum lima</i>	15649
OMWM-2	<i>Prorocentrum minimum</i>	6464
7/28/2023	<i>Kryptoperidinium foliaceum</i>	5443
	<i>Chattonella subsalsa</i>	3742
	<i>Planktothrix agardhii</i>	340
	<i>Karlodinium veneficum</i>	2381
	<i>Lyngbya aestuarii</i> (filament)	340
	<i>Prymnesium parvum</i>	2041
	<i>Amphora fasciola</i>	2381
	<i>Entomoneis paludosa</i>	340
	<i>Neidium smithii</i>	680
	small Naviculoids	680

Table A3 (continued): Algal species and their cell density in the salt marsh ponds (SMPs) samples collected on 7/28/2023, 8/11/2023, and 8/30/2023.

Sample ID	Taxa	Cell density (cells/ml)
SMP00180	<i>Akashiwo sanguinea</i>	580
REF-1	<i>Kryptoperidinium foliaceum</i>	680
8/11/2023	<i>Entomoneis paludosa</i>	120
	<i>Karlodinium veneficum</i>	20
	<i>Levanderina fissa</i>	20
	<i>Bacillaria paxillifer</i>	240
	<i>Prorocentrum lima</i>	20
SMP00182	<i>Karytoperidinium foliaceum</i>	120
REF-2	<i>Alexandrium</i> sp.	60
8/11/2023	<i>Prorocentrum lima</i>	560
	<i>Heterocapsa niei</i>	180
	<i>Prymnesium parvum</i>	440
	<i>Akashiwo sanguinea</i>	140
	<i>Heterosigma akashiwo</i>	600
	<i>Cylindrospermopsis</i> sp.	80
	<i>Melosira moniliformis</i>	1020
	<i>Chroococcus</i>	40
	<i>Chaetoceros tenuissimus</i>	120
	<i>Nitzschia</i> spp.	60
	<i>Lyngbya aestuarii</i> (filament)	20
	<i>Cyclotella atomus</i>	160
	<i>Plesurosigma salinarum</i>	20
	<i>Amphidinium carterae</i>	20
	<i>Amphora fasciola</i>	40
SMP00184	<i>Kryptoperidinium foliaceum</i>	26080
PGD-1	<i>Heterosigma akashiwo</i>	600
8/11/2023	<i>Nitzschia</i> spp.	20
	<i>Planktothrix agardhii</i> (filament)	40
	<i>Chattonella subsalsa</i>	60
	<i>Amphidinium carterae</i>	240
	<i>Heterocapsa niei</i>	100

Table A3 (continued): Algal species and their cell density in the salt marsh ponds (SMPs) samples collected on 7/28/2023, 8/11/2023, and 8/30/2023.

SMP00186	<i>Heterosigma akashiwo</i>	14340
PGD-2	<i>Kryptoperidinium foliaceum</i>	380
8/11/2023	<i>Karlodinium veneficum</i>	860
	<i>Akashiwo sanguinea</i>	460
	<i>Chattonella subsalsa</i>	100
	<i>Amphidinium carterae</i>	980
	<i>Prymnesium parvum</i>	12400
	<i>Anabaena</i> (filament)	20
	<i>Chroococcus</i> sp.	40
	<i>Prorocentrum minimum</i>	40
	<i>Lyngbya aestuarii</i> (filament)	20
	<i>Phormidium autumnale</i>	120
	<i>Nitzschia</i> spp.	60
	<i>Navicula</i> sp	100
	<i>Cyclotella atomus</i>	760
SMP00188	<i>Prorocentrum lima</i>	760
OMWM-1	<i>Chattonella subsalsa</i>	80
8/11/2023	<i>Cylindrotheca closterium</i>	80
	<i>Nitzschia</i> spp.	460
	<i>Chaetoceros tenuissimus</i>	1960
	<i>Alexandrium</i> sp.	200
	<i>Navicula</i> sp.	260
	<i>Heterocapsa niei</i>	200
	<i>Prorocentrum minimum</i>	120
	<i>Lyngbya aestuarii</i> (filament)	20
	<i>Nitzschia longissima</i>	20
	<i>Pleurosigma salinarum</i>	20
SMP00190	<i>Chattonella subsalsa</i>	7700
OMWM-2	<i>Karlodinium veneficum</i>	20
8/11/2023	<i>Heterosigma akashiwo</i>	280
	<i>Amphidinium carterae</i>	480
	<i>Heterocapsa niei</i>	660
	<i>Cyclotella atomus</i>	720
	<i>Cymbella</i> sp.	60
	<i>Alexandrium</i> sp.	100
	<i>Neidium smithii</i>	40
	<i>Prymnesium parvum</i>	540
	<i>Prorocentrum minimum</i>	20
	<i>Prorocentrum lima</i>	80
	<i>Eutreptiella</i> sp.	20

Table A3 (continued): Algal species and their cell density in the salt marsh ponds (SMPs) samples collected on 7/28/2023, 8/11/2023, and 8/30/2023.

Sample ID	Taxa	Cell density (cells/ml)
SMP00192	<i>Akashiwo sanguinea</i>	860
REF-1	<i>Entomoneis paludosa</i>	220
8/30/2023	<i>Krytoferidinium foliaceum</i>	20
	<i>Navicula</i> sp. (>20 um)	20
	<i>Karlodinium veneficum</i>	60
	<i>Cocconeis</i> sp.	20
	<i>Cymbella</i> sp.	60
	<i>Heterocapsa niei</i>	60
	<i>Prorocentrum minimum</i>	20
SMP00194	<i>Alexandrium</i>	180
REF-2	<i>Navicula</i> spp.	1200
8/30/2023	<i>Nitzschia longissima</i>	380
	<i>Akashiwo sanguinea</i>	140
	<i>Licmophora flabellata</i>	160
	<i>Prorocentrum minimum</i>	120
	<i>Prorocentrum lima</i>	100
	<i>Thalassionema frauenfeldii</i>	100
	<i>Karlodinium veneficum</i>	100
	<i>Amphidinium carterae</i>	220
	<i>Prorocentrum lima</i>	20
	<i>Planktothrix agardhii</i> (filament)	60
	<i>Entomoneis paludosa</i>	80
	<i>Chroococcus</i> sp.	160
	<i>Amphora</i> sp.	40
SMP00196	<i>Krytoferidinium foliaceum</i>	22280
PGD-1	<i>Chattonella subsalsa</i>	3000
8/30/2023	<i>Heterocapsa niei</i>	600
	<i>Amphidinium carterae</i>	200
	<i>Phormidium autumnale</i>	20
	<i>Karlodinium veneficum</i>	760
	<i>Entomoneis paludosa</i>	100
SMP00198	<i>Navicula</i> spp.	760
PGD-2	<i>Chattonella subsalsa</i>	900
8/30/2023	<i>Planktothrix agardhii</i> (filament)	20
	<i>Amphidinium carterae</i>	260
	<i>Melosira rubrum</i>	40
	<i>Nitzschia</i> sp.	20
	<i>Heterocapsa niei</i>	300
	<i>Dinoflagellate</i> unidentified	20
	<i>Karlodinium veneficum</i>	160
	<i>Fragilaria gracile</i>	260
	<i>Prymnesium parvum</i>	580
	<i>Prorocentrum minimum</i>	40
	<i>Entomoneis paludosa</i>	20
	<i>Oscillatoria</i> sp.	20
	<i>Calothrix</i> sp.	20
	<i>Thalassiosira tenera</i>	260

Table A3 (continued): Algal species and their cell density in the salt marsh ponds (SMPs) samples collected on 7/28/2023, 8/11/2023, and 8/30/2023.

SMP00200	<i>Prorocentrum lima</i>	640
OMWM-1	<i>Navicula</i> spp.	240
8/30/2023	<i>Heterocapsa niei</i>	320
	<i>Alexandrium</i> sp.	80
	<i>Neidium smithii</i>	80
	<i>Prorocentrum minimum</i>	140
	<i>Staurosira</i> chain	20
	<i>Entomoneis paludosa</i>	20
	<i>Nitzschia sigmoidea</i>	20
	<i>Cymbella</i> sp.	140
	<i>Pleurosigma salinarum</i>	20
	<i>Prymnesium parvum</i>	60
	<i>Navicula rostellata</i>	40
	<i>Karlodinium veneficum</i>	260
SMP00202	<i>Heterocapsa niei</i>	2880
OMWM-2	<i>Karlodinium veneficum</i>	240
8/30/2023	<i>Cymbella</i> sp.	40
	<i>Navicula</i> spp.	240
	picocyanobacteria in clump	60
	<i>Prorocentrum lima</i>	580
	<i>Mastogloia</i> sp.	1600
	<i>Amphora</i> sp.	1280
	<i>Minutocellus scriptus</i>	320
	<i>Nitzschia</i> sp.	20
	<i>Pinnularia</i> sp.	20
	<i>Akashiwo sanguinea</i>	20
	<i>Oocystis</i> sp.	60
	<i>Alexandrium</i> sp.	180
	<i>Prymnesium parvum</i>	720
	<i>Jaaginema</i> sp.	200
	<i>Eutreptiella</i> sp.	20
	<i>Entomoneis paludosa</i>	80
	<i>Prorocentrum minimum</i>	40
	<i>Scriptiella trichoidea</i>	20
	<i>Lyngbya aestuarii</i> (filaments)	20

Table A4: Comparison of algal classifications derived from 18S- and 16S-based DNA sequencing.

	18S-based Classification	16S-based Classification
Algal Groups	Family/Genera/Species	Family/Genera/Species
Chlorophytes	<i>Picochlorum eukaryotum</i>	<i>P. eukaryotum</i>
	<i>Nannochloris atomus</i> , <i>N. maculatum</i>	
	<i>Pyramimonas aurea</i> , <i>P. gelidicola</i> , <i>P. parkeae</i>	<i>Pyramimonas</i>
	<i>Chlorella salina</i>	<i>Chlorella</i>
	<i>Chlamydomonas</i>	<i>Ch. applanata</i> ,
	<i>Tetraselmis marina</i> , <i>T. cordiformis</i>	<i>T. subcordiformis</i> , <i>T. marina</i> , <i>T. cordiformis</i> , <i>T. striata</i>
	<i>Planophila</i>	
	<i>Pterosperma cristatum</i>	<i>Resultor mikron</i>
	<i>Mantoniella squamata</i>	<i>Cyanophora tetracyanea</i>
	<i>Mychonastes</i>	<i>Dunaliella tertiolecta</i>
	<i>Lemmermannia punctata</i>	<i>Coccomyxa subellipsoidea</i>
	<i>Auxenochlorella protothecoides</i>	<i>Picocystis salinarum</i>
	<i>Marvania geminata</i>	<i>Desmochloris halophila</i>
	<i>Urospora</i>	
	<i>Dilabifilum</i>	
	<i>Chlorothrix</i>	Mamiellaceae
	<i>Cladophora</i>	Bathycoccaceae
	<i>Capsosiphon</i>	Scenedesmaceae
	<i>Ulothrix</i>	Prasinophyceae
	<i>Monostroma</i>	Ulvophyceae
	<i>Chlorocystis</i>	
	<i>Pseudendoclonium</i>	
	<i>Hazenia</i>	
Diatoms	<i>Chaetoceros socialis</i> , <i>Ch. spp.</i>	<i>Chaetoceros</i>
	<i>Melosira dubia</i> , <i>M. nummuloides</i>	
	<i>Minidiscus variabilis</i> , <i>M. spinulatus</i>	
	<i>Thalassiosira oceanica</i>	<i>Th. oceanica</i> , <i>Th. pseudonana</i>
	<i>Navicula veneta</i> , <i>N. perminuta</i>	
	<i>Entomoneis</i>	
	<i>Cycloella choctawhatcheeana</i> , <i>C. meneghiniana</i>	<i>Cymatopleura solea</i>
	<i>Planktoniella Sol</i>	<i>Coscinodiscus radiatus</i>
	<i>Amphora capitellata</i> , <i>A. coffeaeformis</i> , <i>A. coffeiformis</i>	<i>Corethron pennatum</i>
	<i>Nitzschia amphibia</i> , <i>N. recta</i>	<i>Cymatosira belgica</i>
	<i>Halamphora subtropica</i>	
	<i>Cymbella cimbebasiae</i>	<i>C. capitata</i> , <i>C. cistuliformis</i> , <i>C. minor</i>
	<i>Rhabdonema adriaticum</i> , <i>R. minutum</i>	<i>Rhizosolenia setigera</i>
	<i>Stauroneis</i>	<i>Asterionellopsis glacialis</i>
	<i>Hyalodiscus</i>	<i>Ditylum brightwellii</i>
	<i>Licmophora</i>	<i>Diatoma tenuis</i>
	<i>Mastogloia</i>	Aulacoseiraceae
	<i>Tryblionella apiculata</i>	Cymbellaceae

Table A4 (continued): Comparison of algal classifications derived from 18S- and 16S-based DNA sequencing.

	18S-based Classification	16S-based Classification
Algal Groups	Family/Genera/Species	Family/Genera/Species
Diatoms	<i>Skeletonema</i>	Dinotrichaceae
	<i>Actinoptychus</i>	Melosiraceae
	<i>Surirella undulatus</i>	Skeletonemataceae
	<i>Pinnularia</i>	Stephanodiscaceae
	<i>Pleurosigma</i>	Thalassiosiraceae
		Fragilariaceae
Cyanobacteria		<i>Lyngbya</i>
		<i>Leptolyngbya</i>
		<i>Phormidium</i>
		<i>Pleurocapsa</i>
		<i>Rivularia</i>
		<i>Raphidiopsis brookii</i>
		<i>Cyanothece</i>
		<i>Merismopedia</i>
		<i>Synechococcus</i>
		<i>Prochlorococcus</i>
		<i>Chroococcus</i>
		<i>Trichodesmium erythraeum</i>
		<i>Planktothrix</i>
		<i>Synechocystis</i>
		<i>Spirulina laxissima</i>
	<i>Calothrix</i>	
	<i>Anabaena</i>	
	<i>Nostoc</i>	
Dinoflagellates	<i>Bysmatrum subsalsum</i>*	
	<i>Heterocapsa niei</i> , <i>H. pygmaea</i> , <i>H. triquetra</i> , <i>H. bohaiensis</i>	
	<i>Prorocentrum</i> <i>cassubicum</i> , <i>P. fukuyoi</i> , <i>P. mican</i> , <i>P. mexicanum</i> , <i>P. texanum</i> , <i>P. triestinum</i>	
	<i>Levanderina fissa</i>	
	<i>Kryptoperidinium foliaceum</i>	
	<i>Barrufeta bravensis</i> , <i>B. resplendens</i>	
	<i>Biecheleria cincta</i> , <i>B. brevisulcata</i>	
	<i>Gyrodinium fusiforme</i>	
	<i>Gymnoxanthea radiolariae</i>	
	<i>Alexandrium andersonii</i> , <i>A. insuetum</i> , <i>A. minutum</i> , <i>A. ostenfeldii</i> , <i>A. tamutum</i>	
	<i>Gymnodinium aureolum</i> , <i>G. litoralis</i>	
	<i>Dinothrix phymatodea</i>	
	<i>Durinskia dybowskii</i>	
	<i>Stoeckeria algicida</i>	
	<i>Pentapharsodinium tyrrhenicum</i>	

Table A4 (continued): Comparison of algal classifications derived from 18S- and 16S- based DNA sequencing.

	18S-based Classification	16S-based Classification
Algal Groups	Family/Genera/Species	Family/Genera/Species
Dinoflagellates	<i>Biecheleriopsis</i>	
	<i>Peridinium</i>	
	<i>Amphidinium carterae</i> , <i>A. steinii</i>	
	<i>Protoperidinium monovelum</i>	
	<i>Gonyaulax spinifera</i>	
	<i>Lepidodinium</i>	
	<i>Archaeoperidinium minutum</i>	
	<i>Paulsenella vonstoschii</i>	
	<i>Ansanella</i>	
	<i>Chimonodinium</i>	
	<i>Breviolum adriatica</i>	
	<i>Chimonodinium lomnickii</i> var. <i>wierzejskii</i>	
	Thoracosphaeraceae	
	Suessiaceae	
Cryptophytes	<i>Chroomonas collegionis</i>	<i>Chroomonas</i>
	<i>Goniomonas amphinema</i>	
		<i>Rhodomonas salina</i>
		<i>Pyrenomonas salina</i>
	<i>Guillardia theta</i>	
Euglenophytes	<i>Eutreptia</i>	<i>E. viridis</i>
	<i>Eutreptiella eupharyngea</i>	<i>E. pomquetensis</i>
		<i>Colacium calvum</i>
		<i>Colacium mucronatum</i>
	<i>Monomorphina pyrum</i>	
Pelagophytes	<i>Aureoumbra geitleri</i>	<i>A. lagunensis</i>
	Sarcinochrysidaceae	Sarcinochrysidaceae
		Pelagomonadaceae
Raphidophytes	<i>Chattonella subsalsa</i>	
	<i>Fibrocapsa japonica</i>	<i>F. japonica</i>
	<i>Chloromorom toxicum</i>	
	<i>Heterosigma akashiwo</i>	<i>H. akashiwo</i>
	<i>Olisthodiscus luteus</i>	
Haptophytes	<i>Pavlova</i>	<i>P. gyrans</i> , <i>P. lutheri</i>
	<i>Diacronema vlkianum</i>	
	<i>Exanthemachrysis</i>	<i>Ochrosphaera</i>
		<i>Emiliana huxleyi</i>
		<i>Phaeocystis</i>
		<i>Chrysochromulina</i>
		<i>Prymnesium</i>
Dictyochophytes	<i>Pseudopedinella elastica</i>	
	<i>Apedinella radians</i>	

Table A4 (continued): Comparison of algal classifications derived from 18S- and 16S- based DNA sequencing.

	18S-based Classification	16S-based Classification
Algal Groups	Family/Genera/Species	Family/Genera/Species
Dictyochophytes	<i>Pteridomonas</i>	
	<i>Ciliophrys infusionum</i>	Dictyochophyceae
	Pedinellales	
Chrysophytes	<i>Chrysowaernella hieroglyphica</i>	
	<i>Paraphysomonas</i>	
	<i>Lepidochromonas</i>	
	<i>Mallomonas caudata</i>	
	<i>Spumella</i>	Chromulinaceae
	Hydrurales	
	Ochromonadales	
Eustigmatophytes	<i>Nannochloropsis gaditana</i> , <i>N. salina</i>	<i>N. gaditana</i>
		Monodopsidaceae

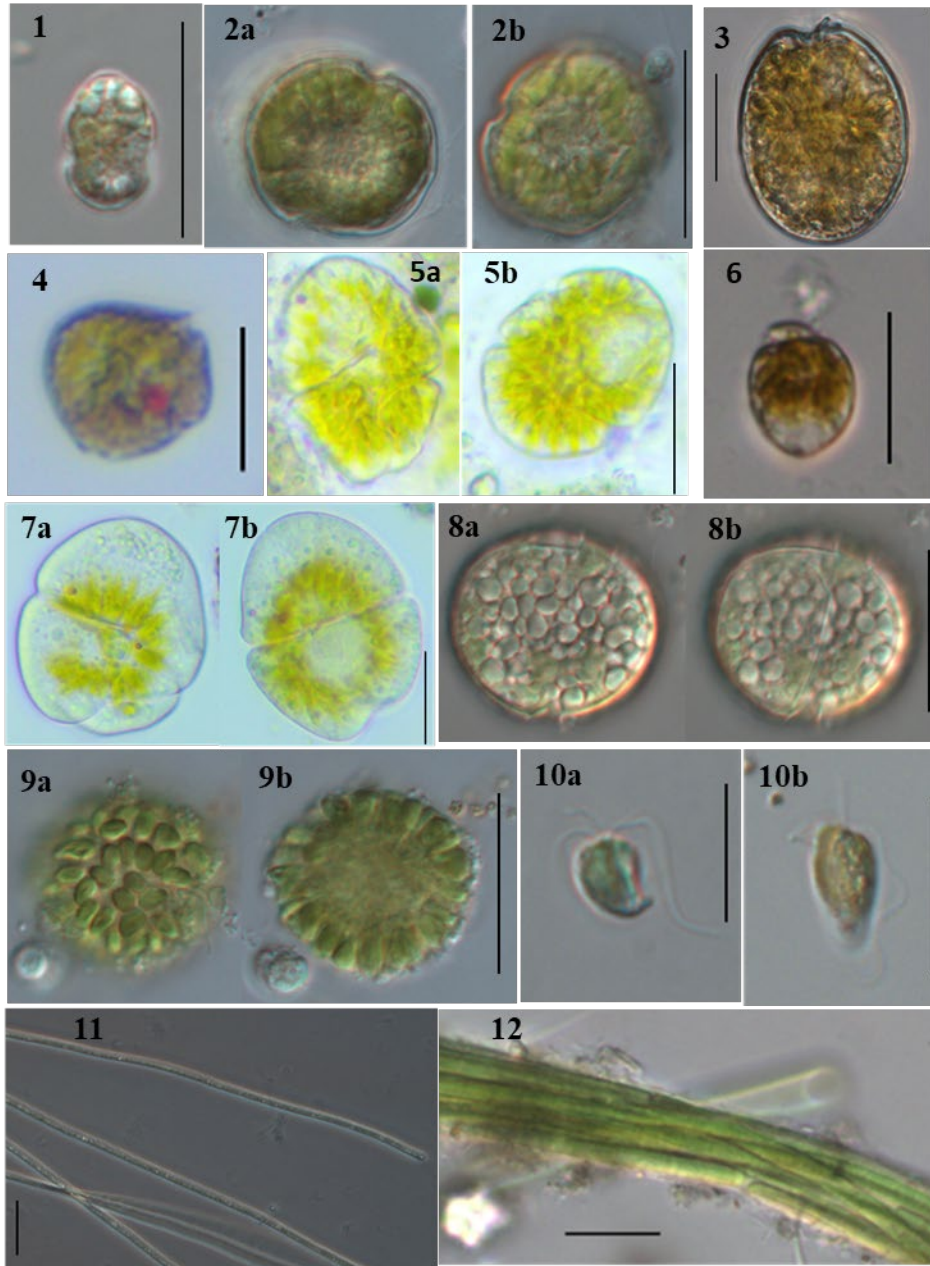


Plate A1 Light micrographs of major harmful algae from salt marsh ponds between June 2022 and June 2023.

1: *Heterocapsa niei*; **2a, 2b:** *Gymnodinium aureolum* (*Karlodinium* sp.), showing nuclei position (a) and the disposition of sulcus (b); **3:** *Prorocentrum lima*; **4:** *Kryptoperidinium foliaceum* (live specimen); **5a, 5b:** *Levanderina fissa* (live specimen); **6:** *Amphidinium caterae*; **7a, 7b:** *Akashiwo sanguinea* (live specimen); **8a, 8b:** dinocysts of *Karlodinium* sp.; **9a, 9b:** *Chattonella subsalsa*; **10a, 10b:** *Prymnesium parvum*, (10b live specimen); **11:** *Planktothrix agardhii* (phase contrast); **12:** *Phormidium autumnale*. Scale bars: 20 μ m.

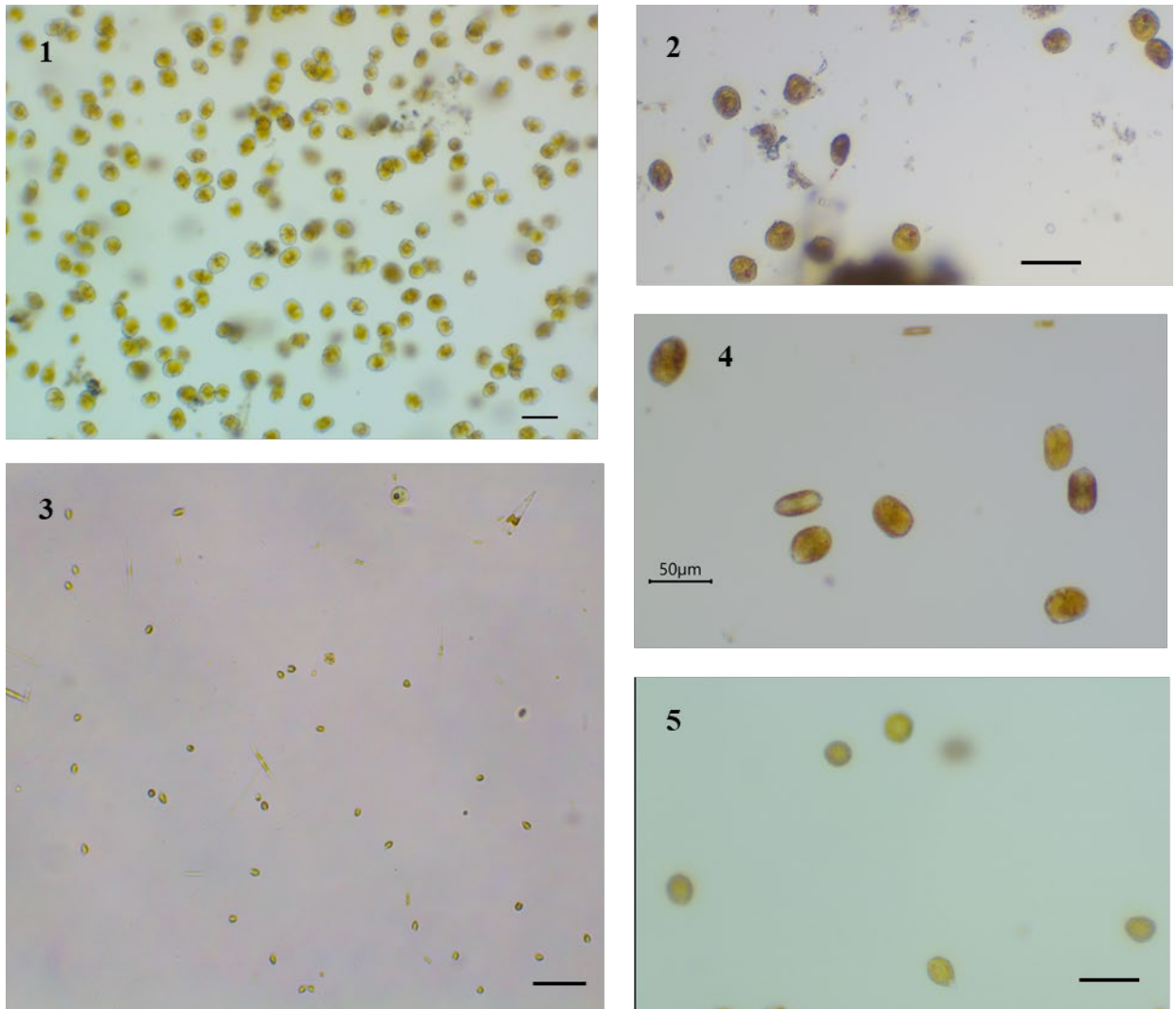


Plate A2 Light micrographs of live samples, showing the dominance of harmful algae in salt marsh ponds, between June 2022 to June 2023.

- 1:** REF-1, July 30, 2022, *Akashiwo sanguinea*;
2: PGD-1, August 24, 2022, *Kryptoperidinium foliaceum*;
3: PGD-2, April 13, 2023, *Prymnesium parvum*;
4: OMWM-1 and OMWM-2, December 7, 2022, *Prorocentrum lima*;
5: OMWM-2, August 24, 2022, *Chattonella subsalsa*.

Scale bars:

- 1:** 100 μm
2-5: 50 μm